SANDIA REPORT

SAND97–2613 • UC–603
Unlimited Release
Printed October 1997

Testing of the AIRRAD Fallout Prediction Code

Mathias J. Sagartz

Prepared by
Sandia National Laboratories
Albuquerque, New Mexico 87185 and Livermore, California 94550

Sandia is a multiprogram laboratory operated by Sandia Corporation, a Lockheed Martin Company, for the United States Department of Energy under Contract DE-AC04-94AL85000.

Sandia National Laboratories

Issued by Sandia National Laboratories, operated for the United States Department of Energy by Sandia Corporation.

Available to DOE and DOE contractors from
Office of Scientific and Technical Information
P.O. Box 62
Oak Ridge, TN 37831

Prices available from (615) 576-8401, FTS 626-8401

Available to the public from
National Technical Information Service
U.S. Department of Commerce
5285 Port Royal Rd
Springfield, VA 22161

NTIS price codes
Printed copy: A04
Microfiche copy: A01

SAND97-2613
Unlimited Release
Printed October 1997

Distribution
Category UC-603

Testing of the AIRRAD Fallout Prediction Code

Mathias J. Sagartz
Experimental Structural Dynamics Department
Sandia National Laboratories
P. O. Box 5800
Albuquerque, New Mexico 87185-0557

Abstract

The origin and basis for the AIRRAD fallout prediction code are reviewed. The model on which AIRRAD is based is described and an earlier implementation of that model, the SIMFIC code, is reviewed. A detailed comparison of SIMFIC and AIRRAD is presented. Three fallout prediction codes, AIRRAD, SIMFIC, and NEWFALL, are exercised to calculate 1 hour normalized dose rates for simple test cases and for five nuclear tests conducted in the atmosphere. The results are used to produce a series of contour plots which provide a basis for comparing the codes with each other and against data for the five atmospheric tests. The report concludes that the current version of the code, AIRRAD 8.1, is a faithful implementation of its underlying model and that its fallout predictions of atmospheric test results are as good or better than the other codes.

Acknowledgments

The author would like to thank Fred Wasmer, author of the original AIRRAD code, for his help in explaining the details of his code and for some historical information about its development. Joe McGahan of Science Applications International Corp. provided very helpful insights into the area of fallout predictions and specifically into the use of his NEWFALL code. Marvin Larsen was invaluable in helping the author understand the AIRRAD source code, and in modifying the code to provide output of intermediate results for comparison with the SIMFIC code equivalents. David Clauss provided many of the figures used in this report and his careful review and suggestions improved the final result. Finally, the author would like to thank Bruce Boughton for his guidance and helpful suggestions throughout the project.

Contents

List of Figures

List of Tables

1 Introduction

Since the advent of nuclear explosives, the prediction of radioactive fallout patterns has been studied extensively. The NEST (Nuclear Emergency Search Team) effects group has chosen an implementation of the SIMFIC model [1] for use in the field to make predictions of nuclear detonation fallout from a terrorist action. To update and tailor the SIMFIC model for it's own use, NEST, along with the U.S. Army Atmospheric Sciences Laboratory, sponsored the development of the AIRRAD code. As the code has been refined and updated over time, several versions have been released. In this report the term AIRRAD is used to refer to AIRRAD 8.1, the current version of the code in use by the NEST effects group. AIRRAD is a fast, state of the art, fallout prediction code with a user friendly interface and graphical output capability. Execution speed is important in NEST applications since effects estimates are needed as quickly as possible in crisis situations. Also, a series of estimates in rapid succession may be required as more accurate estimates of the potential nuclear yield of a terrorist device become available in the field.

The model implemented in AIRRAD is based on the work of H. G. Norment, described in Reference 1. Norment wrote the SIMFIC code to perform calculations based on his fallout model and AIRRAD mirrors the algorithms used by SIMFIC. The user interface and the way the results are handled and output differ between AIRRAD and SIMFIC, but the intent has always been to keep the underlying model the same. The quote below from Reference 1, is Norment's description of his SIMFIC model:

> In SIMFIC [an] altitude-square root of time relationship is used to set up particle trajectory equations in the vertical. These are solved such as to develop equations from which the maximum altitude and the time it is reached can be determined for any particle. With this information along with ambient wind data, horizontal trajectory components are added such as to define the ground impact point for any particle taking into account wind advection throughout the entire period of its rise and settlement. This is done for a sufficient number of representative particles to adequately define the fallout pattern.

This report documents an investigation and the numerical testing that has been done to assure that AIRRAD is a faithful implementation of Norment's SIMFIC model. The first part of the report describes the SIMFIC model, notes some errors and quirks in the SIMFIC code implementation of that model, and compares the AIRRAD and SIMFIC codes. The second part consists of a comparison of fallout calculations from the AIRRAD, SIMFIC, and NEWFALL codes for two idealized problems and for five atmospheric tests.

2 The SIMFIC Model

Norment's model is of a class generally known as "disk tossers." This means that the initial debris cloud caused by a nuclear detonation is modeled as a circular cylinder.

A series of uniformly spaced horizontal planes is used to divide the original cloud into a stack of identical concentric cylinders. The cloud is first defined at the "initial time," which is a time close to fireball second temperature maximum. At that time, the model divides the cloud into a stack of circular cylinders whose radii equal the cloud initial radius as shown in Figure 1. Bounding upper and lower surfaces of the cylinders are referred to as disks. A disk internal to the stack serves as both the upper surface of one cylinder and the lower surface of another, so that the number of disks is always one more than the number of cylinders.

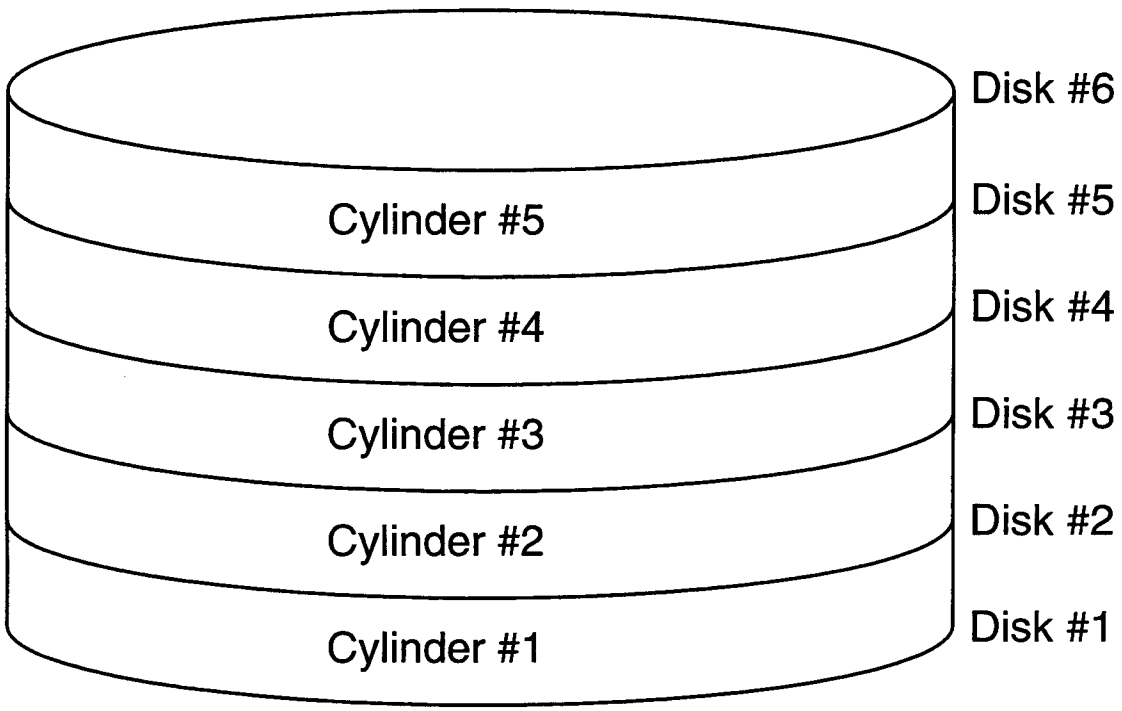

Figure 1: Cylinder stack modeling initial cloud geometry

The mass of fallout is assumed to be uniformly distributed throughout the cloud at the initial time so the contents of each cylinder are identical. After the initial time, the cloud rises and carries the fallout particles along with it. As the cloud rises, some particles fall out of the cloud cap and form the stem part of the "mushroom" cloud. Separate equations are used to describe the trajectories of particles in the stem and those remaining in the cloud cap. The rise speed of particles remaining in the cloud cap differs from that of the cap itself by this settling speed. Ambient winds transport the particles down range as they rise and settle back to earth. Since different size particles settle at different rates, the rise and settling calculations for each of the cylinders must be repeated for each of the particle size classes that are used to represent the fallout debris.

Trajectory calculations are performed for a particle at the center of each disk. As the disks drift with the wind, their lateral growth is modeled based on a measure of ambient turbulence in the cloud. The horizontal distribution of particles, which started out as uniform, is then characterized by a Gaussian distribution whose variance is used to

characterize the "size" of a disk. Eventually, all of the disks settle back to earth and the landing location for the particle at the center of each disk is noted. The particles for each size class in each cylinder are distributed along the ground between the landing locations of their bounding disks. A bivariate Gaussian function, described in Reference 1, is used to distribute the particles in each cylinder between landing locations of its bounding disks.

In his implementation of the SIMFIC model, Norment uses either five cylinders to characterize the debris cloud or calculates the number of cylinders using an algorithm that depends on the detonation yield. He suggests that prediction accuracy does not improve when more than five cylinders are used. SIMFIC uses 75 particle size classes to characterize the cloud debris, but the code has provisions for combining the classes so that calculations can be done using 75, 38, 25, or 19 particle size classes. A table of exposure rate activity fractions is used to distribute the total activity from a detonation among the particle size classes. The table was generated by Norment based on the output of test cases run using the DELFIC fallout model [2]. Data for the size and activity fraction of the particle size classes are given at the end of Appendix A.

SIMFIC calculates an activity distribution on the ground for each cylinder of each particle size class. Total activity is given by summing the contributions of all of the cylinders, i.e., for a calculation using 5 cylinders and 75 particle size classes, 375 contributions are summed to arrive at the fallout activity distribution. It should be noted that Norment has a "ground roughness" input parameter in SIMFIC that he uses to improve the agreement between code output and field measurement data. In Reference 3, Norment states that;

> To compare observed with calculated gamma ray dose rates, it is usually necessary to correct for survey instrument response and ground-roughness absorption. Standard practice is to multiply calculated values by a combined factor of 0.5, ...

Activity decreases with time according to a $t^{-1.26}$ factor, where t is the time after detonation in hours. The total amount of activity produced is linearly dependent on the amount of fission yield in the device, i.e., "K-factor scaling" is used. Norment considers seven different types of fission devices and specifies a different K-factor for each one as shown in Table 1. For a given fission yield, the device type with the highest K-factor produces about 30% more activity than the type with the lowest K-factor.

3 Quirks and Errors Noted in the SIMFIC Code

In the process of this investigation some anomalies and quirks were noted in the SIMFIC code. Because official versions of SIMFIC were never maintained (as far as we were able to determine), the problems noted below cannot be said to exist in "the" SIMFIC code. However, they are in the version of the SIMFIC code obtained from the AIRRAD developers, who received it directly from Norment at the time they began development of AIRRAD (about 1985.)

Fission Type[1]	K-Factor $\frac{R \cdot m^2}{hr \cdot kT}$
P239HE	6.0830×10^9
U233HE	6.3010×10^9
P239FI	6.9733×10^9
U235HE	7.2911×10^9
U235FI	7.8643×10^9
U238TN	7.9407×10^9
U238HE	8.2111×10^9

Table 1: K-Factors for Device Types

Problem 1 The SIMFIC model adjusts the activity created by a detonation for height of burst, HOB. For a given device yield, total activity decreases as HOB increases. The code calculates and lists the correction factor for HOB specified by the model, but never uses that factor to scale its results.

Problem 2 SIMFIC will not run with calm winds. It will, however, run with a small nonzero wind speed at the lowest wind observation point.

Problem 3 The lowest disk in the cloud stack falls out of the cloud immediately at the initial time. If the SIMFIC model predicts that this disk hits the ground before cloud stabilization time, then the SIMFIC model requires that the disk variance (a measure of its size) be set to one half of the initial cloud radius. However, the code sets this variance to twice the initial cloud radius which tends to reduce the concentration of fallout activity deposited very close to ground zero.

Problem 4 There is a discrepancy between the initial cloud base altitude given by Equation (2.6.3) in Reference 1 and the formula used by the code. By checking other references given in Norment's report, it was determined that the expression used by the code is the correct one and Equation (2.6.3) is wrong.

Problem 5 For purposes of calculating cloud advection, the SIMFIC model breaks up the atmosphere into horizontal layers within which the horizontal component of wind velocity is assumed to be constant. Elevations of the data points in the wind profile are used as a basis for defining the wind layers, i.e., their base and top elevations.

The code uses an irrational method for defining wind layers. It begins at ground level and sets the thickness of the first wind layer equal to twice the height of the first wind observation. That is, the elevation of the first wind observation is centered in the first wind layer. The second wind layer is defined by using the same reasoning, with the top of the first wind layer being analogous to ground level and the second wind observation being analogous to the first observation. This process continues until wind layers are defined for all of the data points. Unfortunately, this scheme can lead to extreme distortions of wind layer thicknesses, possibly causing some wind observations to be skipped or to be assigned to layers with negative thicknesses.

[1] U – Uranium, P – Plutonium, HE – High Energy Neutron Fission, FI – Fission Spectrum Neutron Fission, TN – Thermonuclear Fission

As an example, consider the case where wind observations are taken at equally spaced altitudes above ground level. The first wind data point is at elevation H, the second at 2H, the third at 3H, etc. With Norment's wind layer scheme, the lowest wind layer would extend from 0 to 2H, i.e., between the ground and the second wind data point. The second wind layer would have 0 thickness, i.e., go from 2H to 2H, and the third wind layer would extend from 2H to 4H. The effect is to decimate the data by having a zero wind layer thickness for the even numbered wind observations.

It should be noted that this problem was observed in some old SIMFIC output listings that were found during this investigation. These results were from sample calculations provided by a sponsor to the AIRRAD developers.

4 Comparison of AIRRAD with SIMFIC, NEWFALL, and Test Data

Calculations based on the same sets of input data were run with three codes: AIRRAD, SIMFIC, and NEWFALL. Output from the codes was carefully analysed and where differences arose, the source codes were examined to try to pinpoint the cause. Also, the codes were modified by adding statements to output intermediate results, which provided additional data for comparison. Plots and numerical values generated in the process will be presented in the next section. Because the SIMFIC code does not contain input instructions, considerable effort was required to understand its requirements. For the benefit of anyone wanting to run the code, Appendix B contains a set of input instructions for SIMFIC developed by the Author.

The SIMFIC and AIRRAD codes use the same empirical equations to define cloud parameters, the amount of activity and it's distribution among the particle size classes, settling velocity of particles, and vertical trajectory of particles. Examination of intermediate output from the code calculations done during this study shows that they do indeed use/calculate identical values for these parameters and for particle altitude vs. time. AIRRAD scales activity with height of burst according to the equation in the SIMFIC model while the SIMFIC code does not. Also, AIRRAD assigns the correct disk variance to disks that are initially at the cloud base and that impact the ground prior to cloud stabilization.

AIRRAD differs from the SIMFIC model in its treatment of advection. Advection of a particle is essentially a numerical integration of the horizontal wind velocity components at the particle elevation taken over the time the particle remains airborn. As noted above, SIMFIC uses a constant wind velocity in a layer approximation which makes the integration very simple. AIRRAD, on the other hand, uses a Simpson's Rule with end correction method to do the integration. Because of the different treatment of advection and the other differences noted above, in most cases the two codes produce similar but not identical results.

The AIRRAD and SIMFIC codes have different limits on the number of cylinders used to represent the debris cloud and the number of wind layers used for the advection

calculations. Up to five cylinders can be used with AIRRAD while SIMFIC uses five or more cylinders. In practice, however, both codes are almost always run using five cylinders. The version of SIMFIC used in this study was configured to use wind observations at up to 50 elevations while Version 8.1 of the Airrad code uses up to 30 observations. AIRRAD does not use a ground roughness parameter to scale its results, but if necessary, post processing to scale the AIRRAD output is a very simple matter.

Also included in the fallout prediction comparisons discussed in the following sections are results from another code, NEWFALL, which is not based on the SIMFIC model. NEWFALL is developed and maintained by Science Applications International Corp. under the sponsorship of the Defense Special Weapons Agency (formerly Defense Nuclear Agency) and has received wide distribution as a part of two packages of codes, HPAC (Hazard Prediction & Assessment Capability) and CORES (Consolidated Radiation Environment Software). NEWFALL, like AIRRAD, is a "disk tosser", but it includes features, e.g., the ability calculate fallout from multiple detonations, that show it was written with a view toward military battlefield simulations.

4.1 SIMFIC Qualification

Before making detailed numerical comparisons between AIRRAD and SIMFIC, it must be established that the SIMFIC code used here is a valid version and is working correctly. Fortunately, Reference 1 contains contour plots of one hour normalized dose rate[2] made by Norment using his SIMFIC code for 5 atmospheric tests described in References 3, 4, and 5. The plots in the Reference 1 were digitized and overlaid on contour plots made from our SIMFIC output for these tests. Figures 2–7 show the results. It should be noted that there is some uncertainty that the input data used for the calculations are exactly the same as the data used to generate the curves of Reference 1. In both cases, 5 cloud subdivisions and 19 (every fourth) particle size classes were used. However, the device type, which influences the total amount of fallout activity, was not specified in the reference.

Our calculated SIMFIC results shown in Figure 2 for Small Boy, Figures 3 and 4 for Buster Jangle Sugar, Figure 5 for Johnie Boy, and Figure 6 for Koon, all use the P239FI device type simply because it gives the best agreement with the report contours. The U238HE device type is used for the Zuni calculation, shown in Figure 7, for the same reason, although in this case the agreement is not as good as for the other four tests. Following Norment, a ground roughness parameter of 0.5 was used for all test cases except Zuni where 1.0 was used. Meteorological data used here and in Reference 1 should be the same since both used published results given in References 4 and 5. However, there is no guarantee that the complete weather data sets, which include a few extrapolated values for some of the tests, were used. Winds for the Small Boy test are an exception because they were taken from the "reconstructed" winds given by Norment in Reference 3.

[2]Normalized dose rate is the dose rate that would exist if all fallout were already on the ground regardless of its actual deposition time.

Distance= d (m)	SIMFIC		AIRRAD	
	1 Hr dose rate	1 – 12 hr dose	1 Hr dose rate	1 – 12 hr dose
0	9918	18140	13900	25430
250	1740	3168	1548	2818
500	466.3	837.9	469.8	843.9
750	234.6	414.4	238.4	420.9
1000	140	242.1	141.7	244.8
2000	33.33	50.73	33.39	50.65
3000	12.37	16.05	12.29	15.83
4000	5.747	6.475	5.685	6.316
5000	3.023	3.055	2.98	2.949
6000	1.704	1.585	1.677	1.521
7000	0.9974	0.8695	0.9756	0.8247

Table 2: Dose Rate (R/Hr) and Accumulated Dose (R), 1 kT Fission Device, No Wind

Appendix C lists the data used to prepare the test case inputs for both AIRRAD and SIMFIC.

Overall, agreement between the contours presented in Reference 1 and those from our SIMFIC calculations is quite good and supports our belief that the SIMFIC code used here is a valid, legitimate version.

4.2 Code Comparisons for Simple Test Cases

The ideal situation for establishing AIRRAD as an implementation of the SIMFIC model would have been to have a code that was a validated implementation of the model as described in Reference 1 to compare against. Unfortunately, as pointed out above, this was not the case. Nevertheless, for detonations with a low HOB and where winds don't change rapidly with elevation, we would expect that there should be close agreement between results predicted by the version of the code we obtained and AIRRAD, at least in the far field. The first code comparisons are taken from results for simple test cases, a 1 kT, P239HE fission device and either calm winds or winds that are constant in both speed and direction. As noted above (see Problem 2 in Section 3), SIMFIC will not run with absolutely calm winds, but by using a very low wind speed in a single thin layer, results were obtained for an effectively zero wind case. Calculations for the test cases were done using 5 cloud subdivisions, all 75 particle size classes and a ground roughness parameter of 1. Table 2 shows the results at various distances from ground zero in the no wind case. Height of burst was taken as 2 meters, so the SIMFIC results in the table are actually the code output multiplied by 0.92327, the HOB scaling factor from the SIMFIC model. As expected, both the 1 to 12 hour accumulated dose and the 1 hour normalized dose rate results show very good agreement except (see Problem 3 in Section 3) near ground zero.

The second test case is similar to the first except that a 0 HOB was used and

Distance= d	SIMFIC		AIRRAD		NEWFALL	
(m)	$-x = y = d$	$x = 0\ y = d$	$-x = y = d$	$x = 0\ y = d$	$-x = y = d$	$x = 0\ y = d$
0.	4254	4254	5813	5813	2700000	2700000
250.	2704	1290	3165	1101	2900	2400
500.	1243	205.5	1349	172.4	1400	600
750.	774.1	74.16	755.3	69.73	930	110
1000.	536.7	42.38	523.3	41.5	630	0
1250.	399.8	27.54	391.1	26.66	460	0
1500.	307.4	18.95	300.5	18.14	310	
1750.	241.2	13.59	236.1	12.99	250	
2000.	193.4	10.08	189.1	9.593	190	
2500.	131.5	5.94	128.7	5.63	120	
3000.	94.56	3.74	92.49	3.5	81	
3500.	70.69	2.49	69.08	2.29	61	
4000.	54.34	1.75	53.14	1.60	45	
4500.	42.65	1.29	41.68	1.18	36	
5000.	34.05	0.993	33.27	0.91	28	
6000.	22.68	0.645	22.2			
7000.	15.87	0.456	15.5			
8000.	11.53	0.340	11.3			
9000.	8.605	0.216	8.4			
10000.	6.523	0.204	6.4			

Table 3: 1 Hr. Normalized Dose Rate (R/Hr), 1 kt, $v_y = -v_x$ =1 m/s

velocity is $v_y = -v_x = 1$ m/s at all altitudes. Table 3 shows the results for normalized one hour dose rate and again SIMFIC and AIRRAD results show good agreement except very close to ground zero. Contour plots from the results, shown in Figure 8, confirm the close agreement. Also included in the table are results calculated with the NEWFALL code. These results were obtained using the standard parameter set furnished with NEWFALL[3]. In particular, the default "K-factor" which relates total fallout activity to fissile yield is about 34% higher in NEWFALL than the "K-factor" used by AIRRAD and SIMFIC for a P239HE device type. An important difference between the standard version of NEWFALL and AIRRAD is that NEWFALL calculates a sharply defined fallout area for its disks and uniformly distributes the fallout within this area rather than using the smooth Gaussian distribution specified by the SIMFIC model. As a result, NEWFALL contours have a more ragged appearance than those generated by codes using Gaussian distributions[4]. AIRRAD and NEWFALL contours, shown in Figure 9, illustrate how this difference changes the 10, 25, 100, 500 and 2000 R/Hr normalized dose rate fallout contours for the second test case.

[3]The NEWFALL code comes with a default set of parameters, however most of these can be easily changed by the user.

[4]A version of NEWFALL using Gaussian rather than uniform distributions for fallout is also available.

4.3 Code Comparisons for Atmospheric Tests

For further comparisons, the same five test cases from Reference 1 that were used to "validate" our version of SIMFIC were used again. All of the SIMFIC results, with one exception noted below, were obtained by using the code "as is" with no attempt to correct any of the inconsistencies noted between the model documentation and the coding. However, some scaling of the AIRRAD and SIMFIC results was done so that equivalent test cases were being compared. Scaling is necessary because AIRRAD does not include a ground roughness factor but it does use a height of burst correction for total activity. AIRRAD results for dose rate are multiplied by the ground roughness factor used in the SIMFIC calculation while SIMFIC results are multiplied by the height of burst correction factor. Figures 10–20 show overlays of contour plots from SIMFIC and AIRRAD as well as contour plots from NEWFALL for the five tests. NEWFALL results were calculated using its standard 50 particle size classes and 12 cloud subdivisions, and were scaled in the same way as the AIRRAD results. The AIRRAD and SIMFIC calculations were done using 5 cloud subdivisions, 75 particle size classes, and ground roughness factor of 0.5, except for the Zuni test which used a ground roughness factor of 1. Because the previous SIMFIC calculations (used to compare with the published results) were done using only 19 particle size classes and were not scaled by the correction factor for HOB, the SIMFIC contours shown here differ slightly from those in Figures 2–7.

Inspection of results for the three low yield NTS (Nevada Test Site) tests, shown in Figures 10–16, shows very good SIMFIC–AIRRAD agreement for the Small Boy and Johnie Boy tests and fair agreement for the Buster Jangle Sugar test. Expected differences in the code results near ground zero can be seen by carefully observing the contours of Figures 10 and 13 in the upwind direction. The more global differences for Buster Jangle Sugar shown in Figures 12 and 13 demonstrate what can happen to SIMFIC calculations when variable winds are combined with poorly chosen wind layer thicknesses. At elevations below 6000 m, Buster Jangle Sugar wind data points are given at 656.2 m (2000 ft) increments, but the SIMFIC code uses wind layer thicknesses that alternate between 170.4 m and 1048.8 m. The one wind data point, at 1829 m elevation, having a westerly velocity component lies in one of the thicker wind layers and exaggerates the tendency of the SIMFIC contours to bend to the west in the vicinity of ground zero. A similar problem also shows up in the calculations for the intermediate yield level test, Koon. For this test, Figure 17 shows AIRRAD contours that tend more toward the east and don't extend out as far as their SIMFIC counterparts.

To illustrate the effect of the SIMFIC code wind layering problem, the code was modified to use a different wind layering scheme. The dividing elevations between the wind layers were chosen to be at the halfway points between wind observations. Contours calculated with the modified SIMFIC code are the dotted lines in Figure 17 and show much closer agreement with the AIRRAD results. The SIMFIC modified contours still go out somewhat farther than the AIRRAD contours, but the overall direction of the fallout pattern shows very good agreement.

Figure 19 shows the code comparison for a high yield test, Zuni. Here the agreement

is good, although again the AIRRAD contours tend to be rotated slightly to the east relative to the SIMFIC contours, again probably due to the way SIMFIC chooses its wind layers.

To avoid cluttering the figures showing SIMFIC vs. AIRRAD comparisons, separate figures are used to show the AIRRAD vs. NEWFALL comparisons. It should be noted that performing the NEWFALL calculations for the tests done at NTS is not straightforward. The difficulty exists because the AIRRAD and SIMFIC calculations assume a flat earth at the ground zero elevation. However, when no terrain map is given, NEWFALL assumes that the elevation of the ground is sea level, which is not the case for the NTS tests. To circumvent this problem, the calculations were done without a terrain map but the barometric pressure input was altered so that the pressure at zero elevation was actually the pressure appropriate for the elevation at ground zero[5]. The NEWFALL calculations were done using all of the code default parameters, including its relatively high estimate for total fallout activity. As expected, the NEWFALL contour plots are relatively jagged, but in general they show reasonably good agreement with AIRRAD calculations. The most noticeable differences occur for the higher yield tests, Koon and Zuni. The NEWFALL contours for Koon tend to extend farther, by about 20%, and more westerly than the AIRRAD contours. For Zuni, the contours appear to have the same orientation, but the NEWFALL contours are not as wide.

4.4 Code Comparisons with Measured Test Data

A final series of plots, showing 1 Hour normalized dose rate contours from AIRRAD predictions and from the test data presented in Reference 1, are shown in Figures 21–25. Because the AIRRAD and SIMFIC codes give very similar results, Norment's comments and conclusions, presented in Reference 1, about the adequacy of SIMFIC are also applicable to AIRRAD. For that reason, and in deference to Norment's considerable experience in the field, his discussion is essentially repeated verbatim here. The only modifications made are that data analysis information specific to this study has been added and some material not of direct interest here has been omitted.

Statistical data derived from the contour plots is shown in Tables 4 and 5. [The DELFIC results shown in the table are taken directly from Reference 1 but the SIMFIC results were recomputed using 75 particle size classes.]

Prediction accuracy is seen to be good, particularly for the low yield shots. Overall mean absolute percent errors[6] for contour area and hotline length[7] are [5 tests combined]:

[5]This work-around was suggested by Joe McGahan, the author of NEWFALL.

[6]For n observed-predicted pairs, mean absolute percent error is

$$\frac{100}{n}\sum_{i=1}^{n}\frac{|x_{obs,i}-x_{pred,k}|}{x_{obs,i}}.$$

[7]Hotline length is defined as the furthest distance from ground zero on a contour.

Test Shot Level (R/Hr.)	Area (km^2)				
	Test	AIRRAD	SIMFIC	DELFIC	NEWFALL
Small Boy					
50	9.03	6.041	6.621	4.38	8.172
100	3.75	1.798	1.925	1.1	2.83
200	0.942	0.7833	0.9463	0.564	1.084
500	0.528	0.2817	0.3288	0.135	0.3187
1000	0.216	0.1186	0.1143	0.047	0.1805
mean % error		39 (37)	32 (28)	63 (59)	21 (22)
Jangle-Sugar					
35	3.114	3.495	3.094	5.077	7.567
100	1.437	1.082	1.207	2.242	2.162
300	0.386	0.3303	0.428	0.316	0.4339
500	0.117	0.1624	0.1647	0.144	0.2035
mean % error		23 (17)	17 (9)	40 (46)	70 (69)
Johnie Boy					
50	1.271	1.337	1.655	1.787	2.236
100	0.539	0.593	0.7233	0.774	0.9522
1000	0.278	0.04068	0.0313	0.029	0.018
mean % error		34 (8)	51 (32)	58 (42)	82 (76)
Koon					
100	550	353.5	368.3	261	442.8
250	122	108.1	112.5	87.3	176.9
500	32	42	42.96	26	93.98
mean % error		26 (24)	25 (20)	33 (40)	86 (32)
Zuni					
30	10950	14890	15550	9913	11700
50	6187	9547	9852	6660	7391
100	2761	4755	4823	3619	4053
150	474	2989	3000	2239	2834
mean % error		173 (54)	177 (59)	105 (16)	143 (24)

Table 4: Observed and Predicted Fallout Contour Areas

	AIRRAD	SIMFIC	DELFIC	NEWFALL
Contour Areas	61 (30)	61 (30)	61 (42)	77 (42)
Hotline Length	24 (18)	27 (17)	32 (26)	35 (27)

The quantities in parentheses are computed with the data for the highest activity level contours excluded. The highest level contours are particularly difficult to predict, usually being in the region affected by throwout and induced activity in and around the crater. The codes do not address this portion of the activity field since fallout is a negligible contributor to casualties there.

For the five tests studied, AIRRAD is shown to be as good as or better than the other codes (SIMFIC, NEWFALL, and DELFIC) in prediction accuracy. It is important

Test Shot	Hotline Length (km)				
Level (R/Hr.)	Test	AIRRAD	SIMFIC	DELFIC	NEWFALL
Small Boy					
50	8.1	7.689	7.755	6.47	7.7
100	5.66	3.666	3.411	3.72	4.048
200	2.22	2.003	2.067	1.69	1.627
500	1.62	1.028	1.056	0.56	0.548
1000	1	0.5675	0.5248	0.25	0.3689
mean % error		26 (22)	27 (21)	44 (36)	38 (32)
Jangle-Sugar					
35	5.06	8.109	5.71	7.68	9.959
100	3.74	3.911	3.556	5.87	3.762
300	1.5	1.776	2.114	1.23	1.023
500	0.69	1.027	1.347	1	0.386
mean % error		33 (28)	38 (20)	43 (42)	43 (43)
Johnie Boy					
50	4.1	4.634	4.861	4.13	4.142
100	2.73	2.408	2.644	2.58	2.141
1000	1.38	0.4866	0.456	0.32	0.09996
mean % error		30 (12)	30 (11)	28 (3)	38 (11)
Koon					
100	41	36.63	41.37	39.5	45.02
250	17.3	20.84	23.75	24.2	25.92
500	10.2	13.15	15.11	12.5	17.46
mean % error		20 (16)	29 (19)	22 (22)	44 (30)
Zuni					
30	177	174.9	188.8	153	186.2
50	138	138.1	147	121	143.2
100	125	96.37	100.2	96	92.33
150	98	76.48	79.54	78	72.26
mean % error		12 (8)	13 (11)	17 (16)	15 (12)

Table 5: Observed and Predicted Fallout Contour Hotline Lengths

to emphasize that this level of competency in AIRRAD has been achieved without a posteriori adjustment or calibration of any aspect of the model so as to improve agreement with any particular observed fallout pattern.

The three low yield shots were executed at the Nevada Test Site, and their fallout patterns were measured over land. For this reason, observed patterns for these shots, though not highly accurate, may be considered to be superior to the patterns of the high yield shots which were executed on Bikini Atoll in the South Pacific. Not only are the fallout fields of the high yield shots very large, which adds to measurement problems, but most of the fallout from these shots fell into water. Even so, most of the Koon pattern area was covered by an array of fallout collection stations, so this pattern is probably reasonably accurate. Zuni, on the other hand, is a special case. The fallout pattern used here is exclusively downwind of the atoll and was determined by an oceanographic survey

method that was known to be inaccurate. The close-in pattern in the region of the atoll is available, but contains no closed contours so could not be used here; thus the high-activity portion of the observed pattern for this shot is ignored, and this alone must account for a substantial portion of the disagreement between observation and prediction for this shot, particularly with regard to contour areas.

Predictions for these high yield shots are expected to be inferior to those for these low yield shots. This is because both of the high yield shots were detonated over coral soil, and in the case of Zuni, a large but uncertain amount of sea water was lifted by the cloud. The particle size distribution used for these predictions is typical of fallout produced from the siliceous soil found at the Nevada Test Site. We have not succeeded in developing a distribution appropriate for coral and coral-sea water mixtures.

More details concerning the prediction calculations and test shot characteristics are in Reference 3.

5 Conclusions

In the process of reviewing the manuals and documentation for AIRRAD and SIMFIC, nothing was found that indicates any deviation of the AIRRAD code from Norment's SIMFIC model. In fact, AIRRAD corrects some problems that exist in Norment's coding of his model. Detailed numerical comparisons indicate that the AIRRAD and SIMFIC codes are essentially the same except for the the algorithms used to calculate advection of the fallout. Because of the flawed way that the SIMFIC code defines wind layers, it can produce a poor model for advection and noticeable differences can exist between its results and those calculated using AIRRAD. In spite of this problem, calculations for zero wind and constant wind test cases and for five above ground nuclear tests show that AIRRAD and SIMFIC produce results that are usually in good agreement. Probably the best way to regard the AIRRAD code is as a corrected and updated version of the SIMFIC code. The good general agreement between AIRRAD and NEWFALL results provides an additional measure of confidence in AIRRAD's ability to predict fallout patterns.

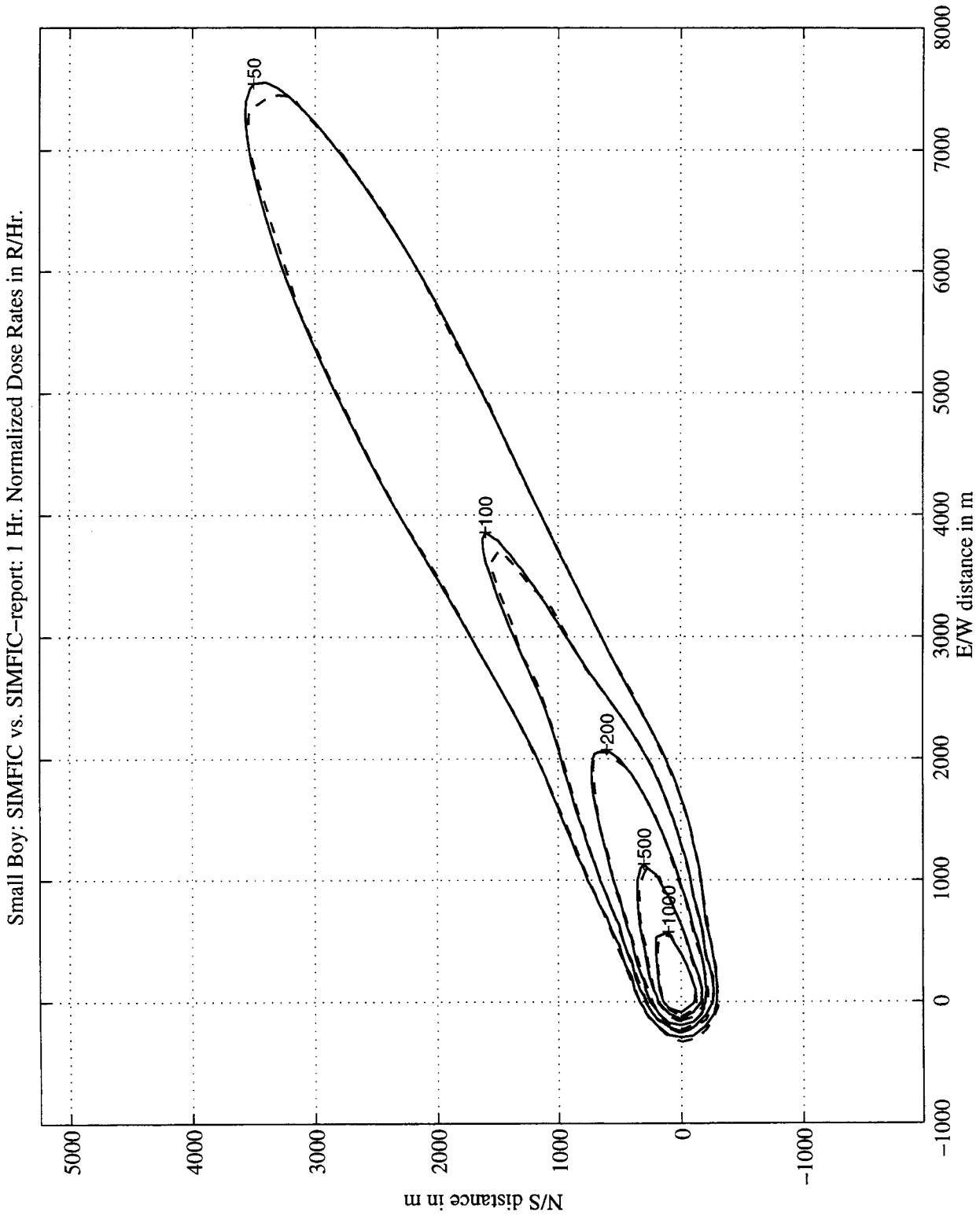

Figure 2: Small Boy contours, calculated (solid) vs. report

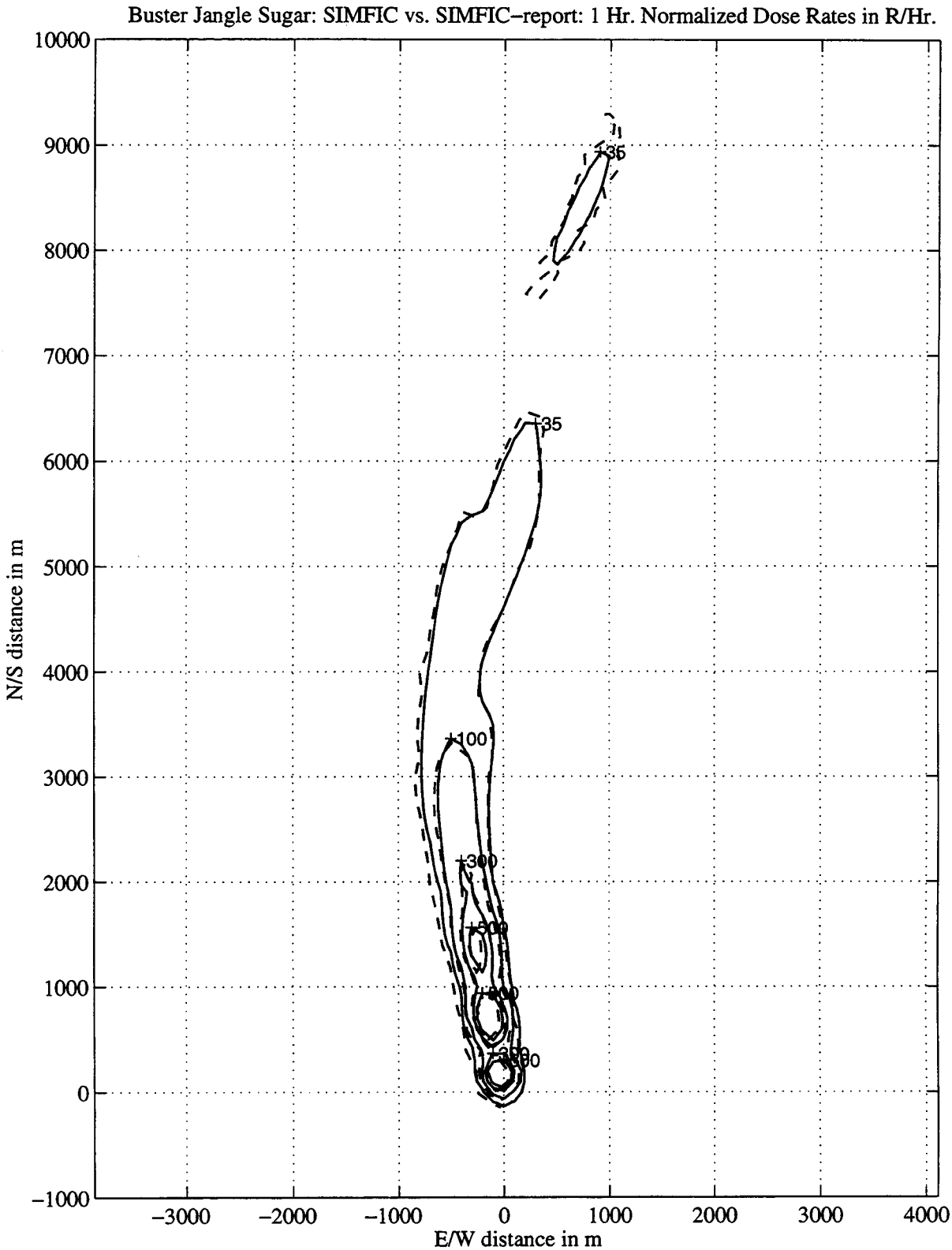

Figure 3: Buster Jangle Sugar full contours, calculated (solid) vs. report

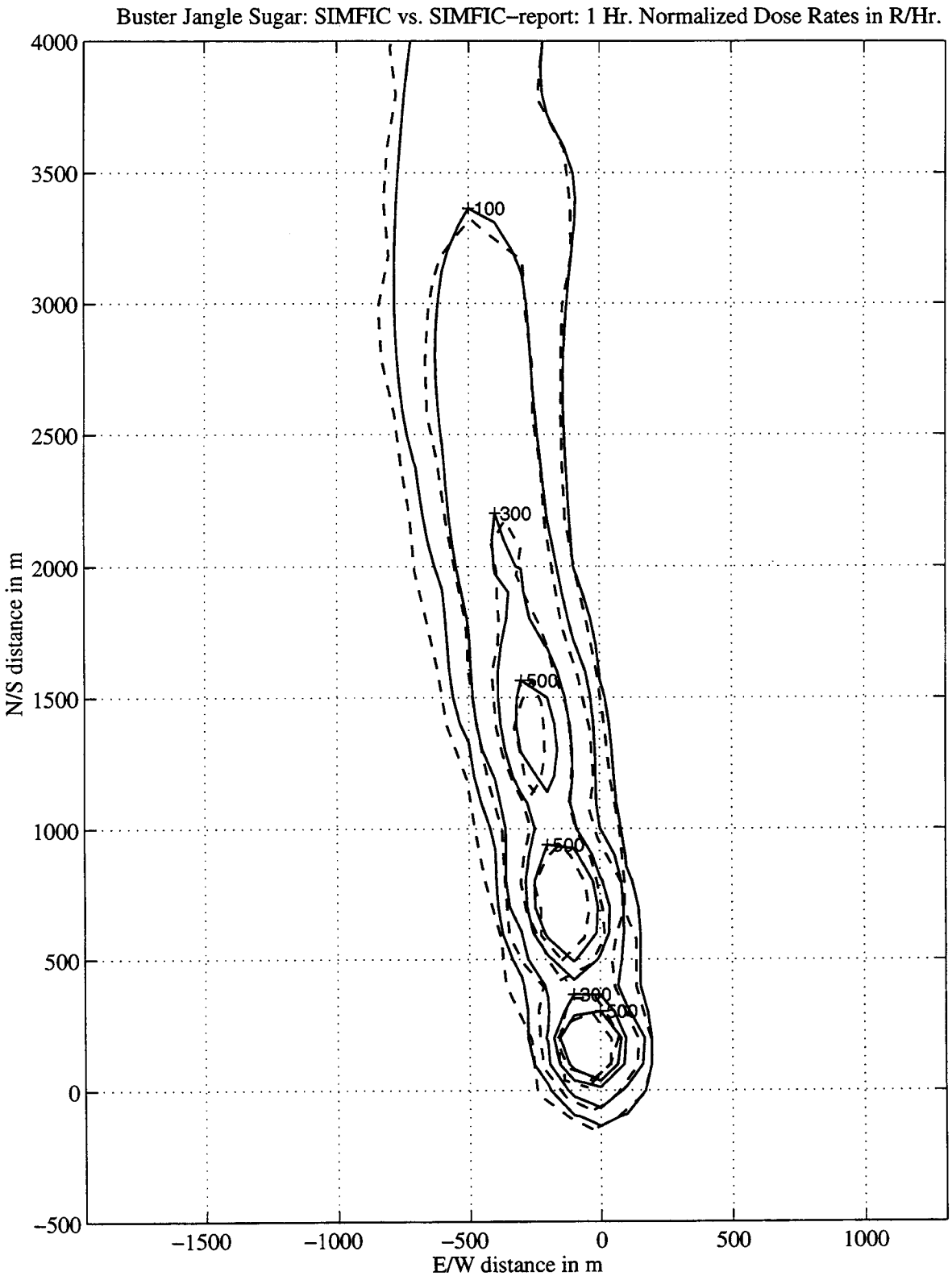

Figure 4: Buster Jangle Sugar partial contours, calculated (solid) vs. report

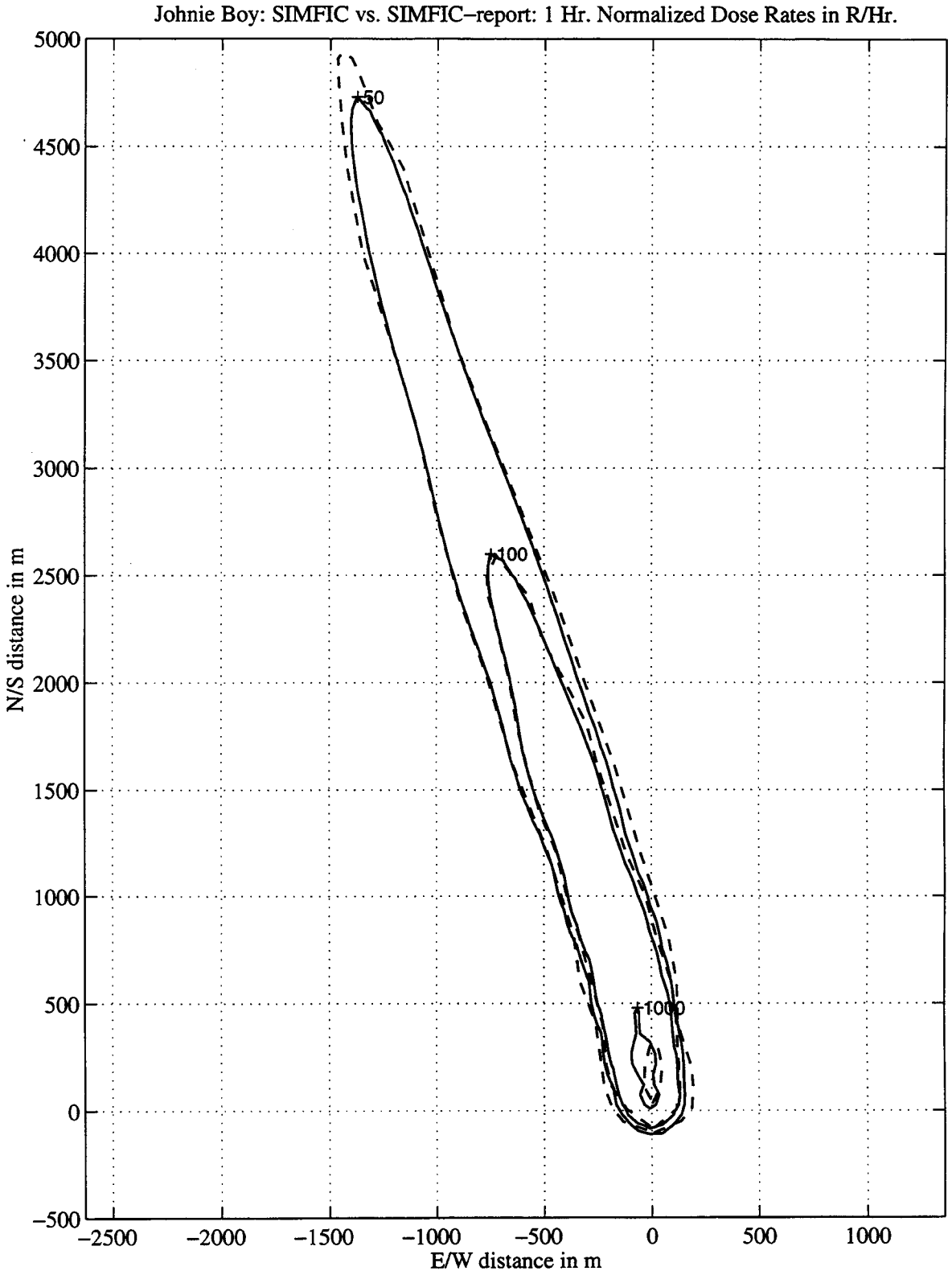

Figure 5: Johnie Boy contours, calculated (solid) vs. report

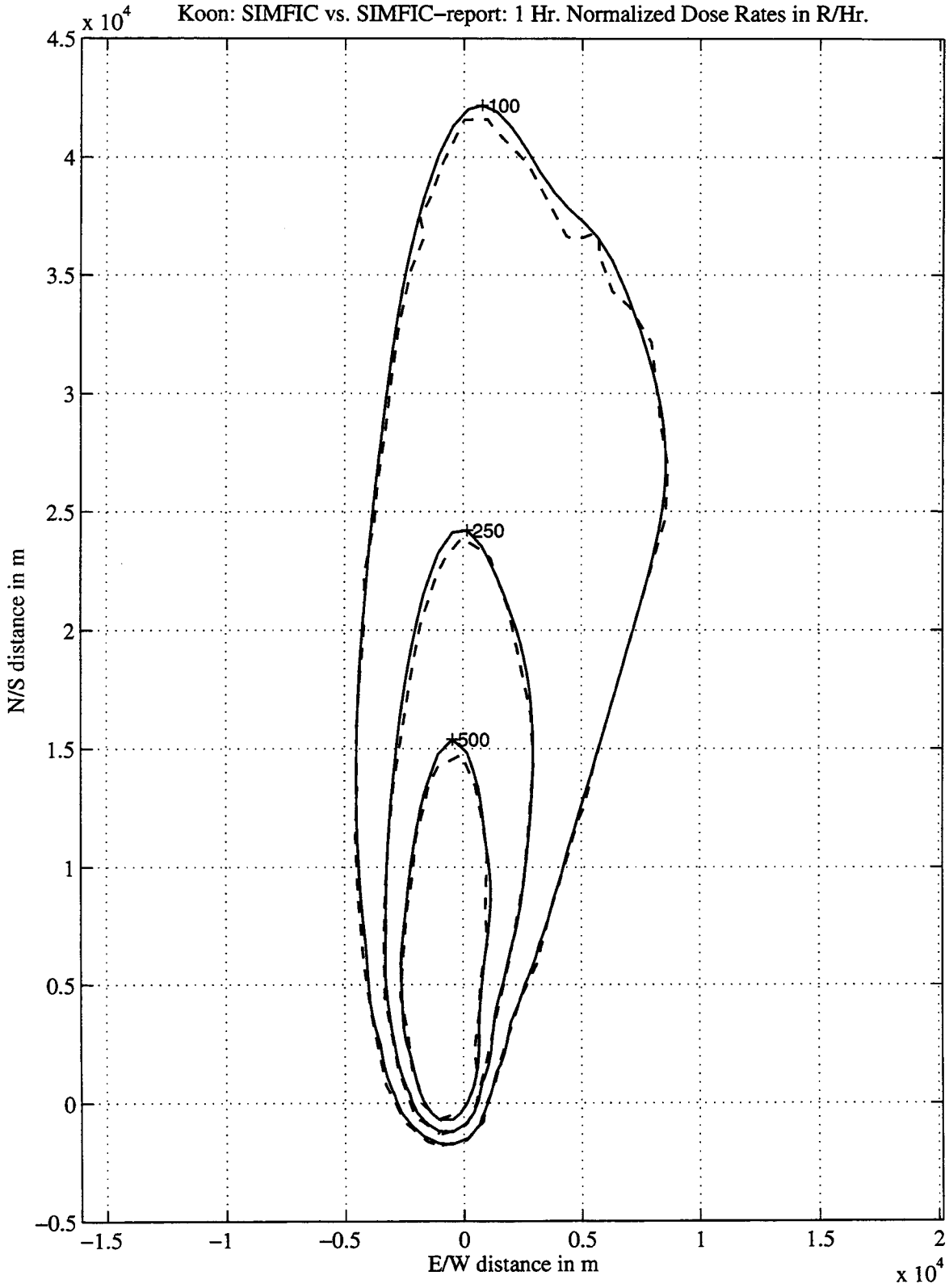

Figure 6: Koon contours, calculated (solid) vs. report

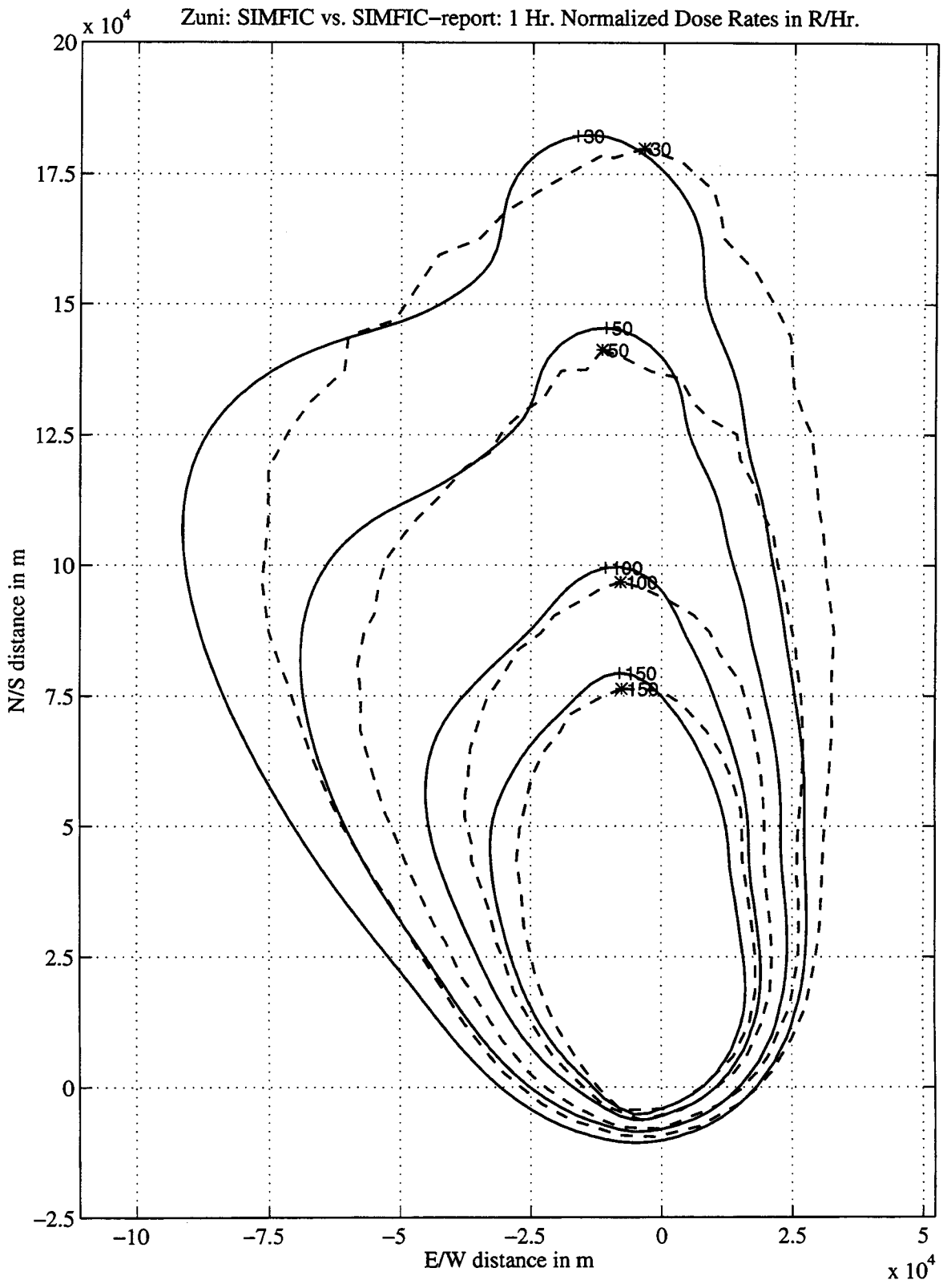

Figure 7: Zuni contours, calculated (solid) vs. report

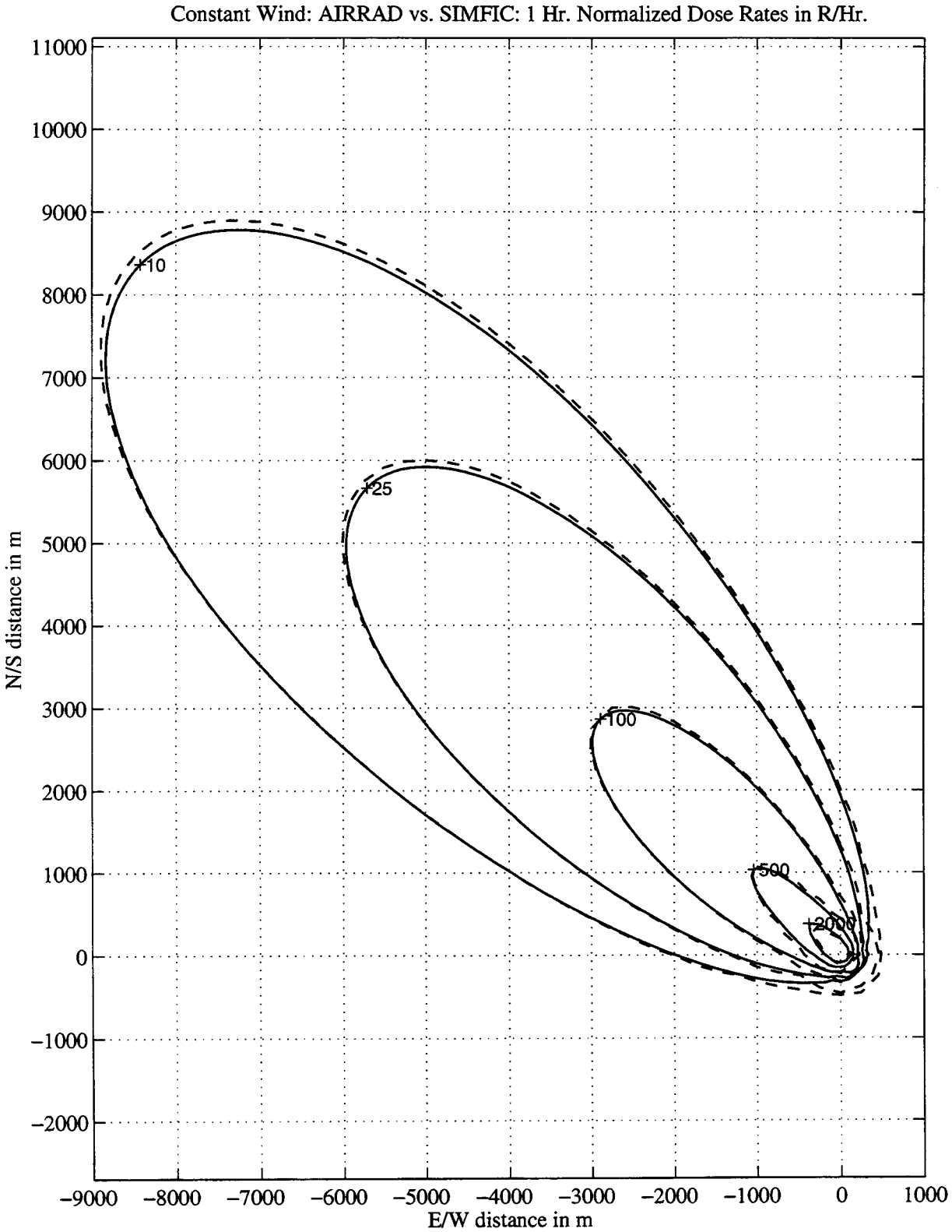

Figure 8: Unit Wind contours AIRRAD (solid) vs. SIMFIC (dashed)

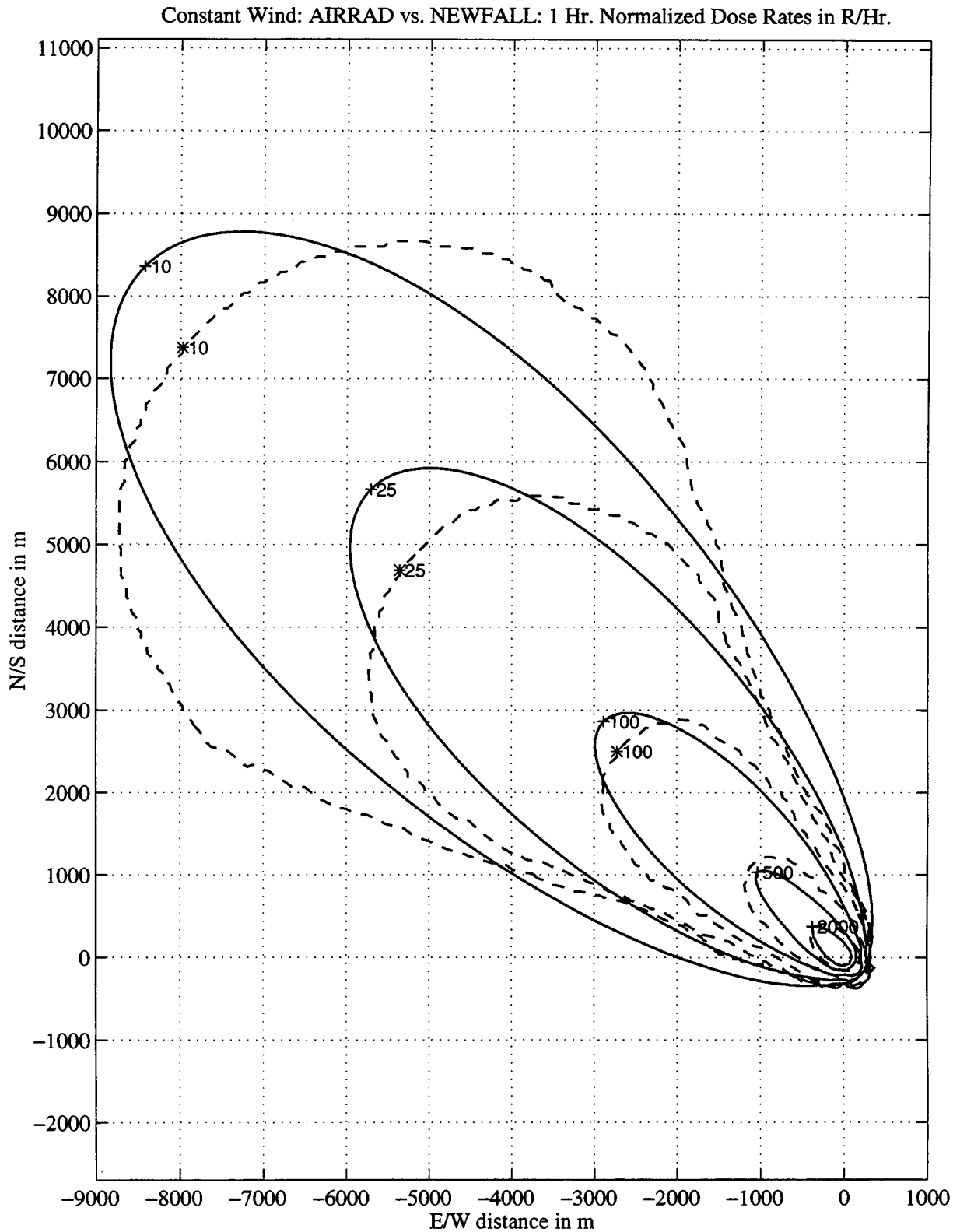

Figure 9: Unit Wind AIRRAD contours (solid) vs. NEWFALL (dashed)

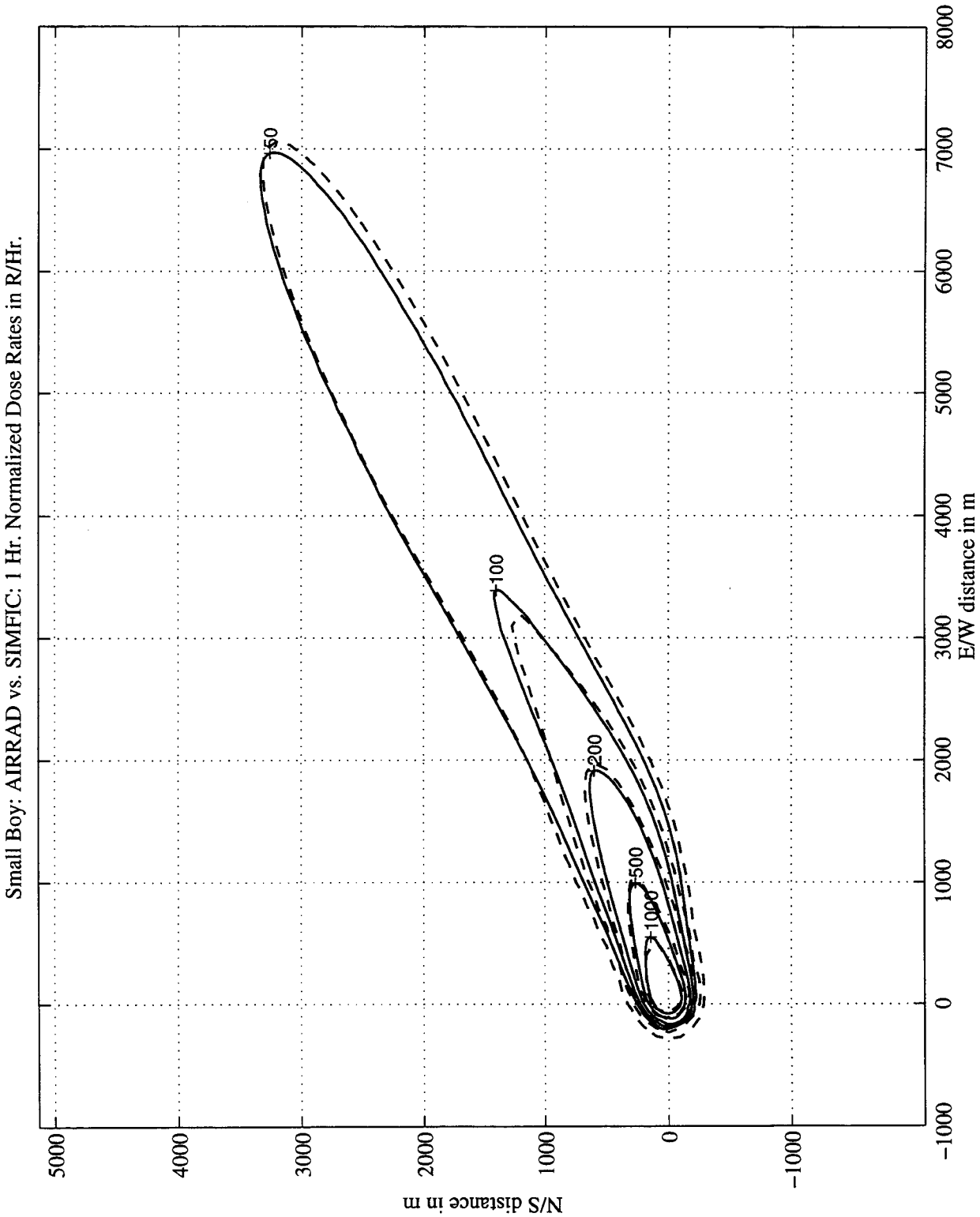

Figure 10: Small Boy contours, AIRRAD (solid) vs. SIMFIC (dashed)

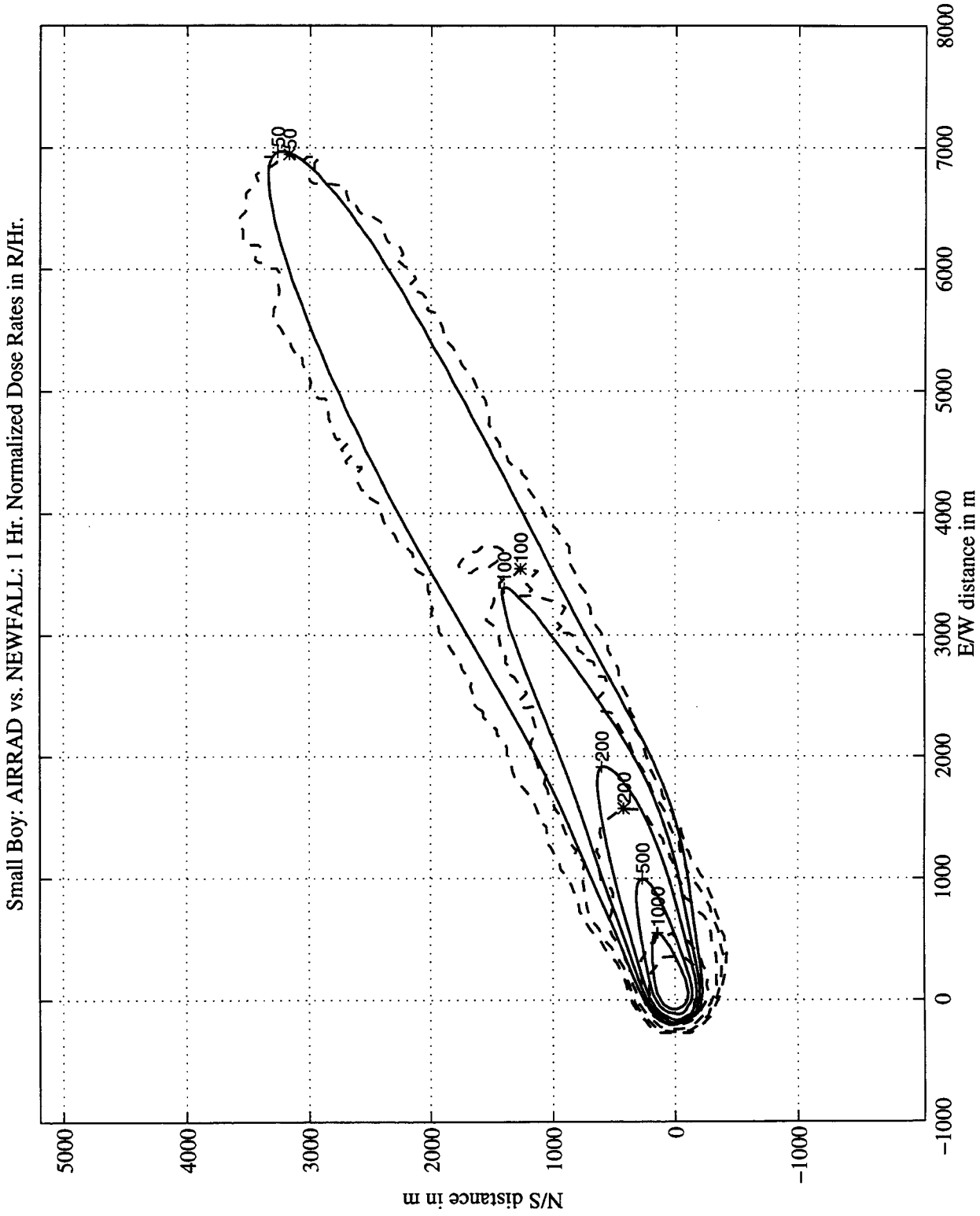

Figure 11: Small Boy contours, AIRRAD (solid) vs. NEWFALL (dashed)

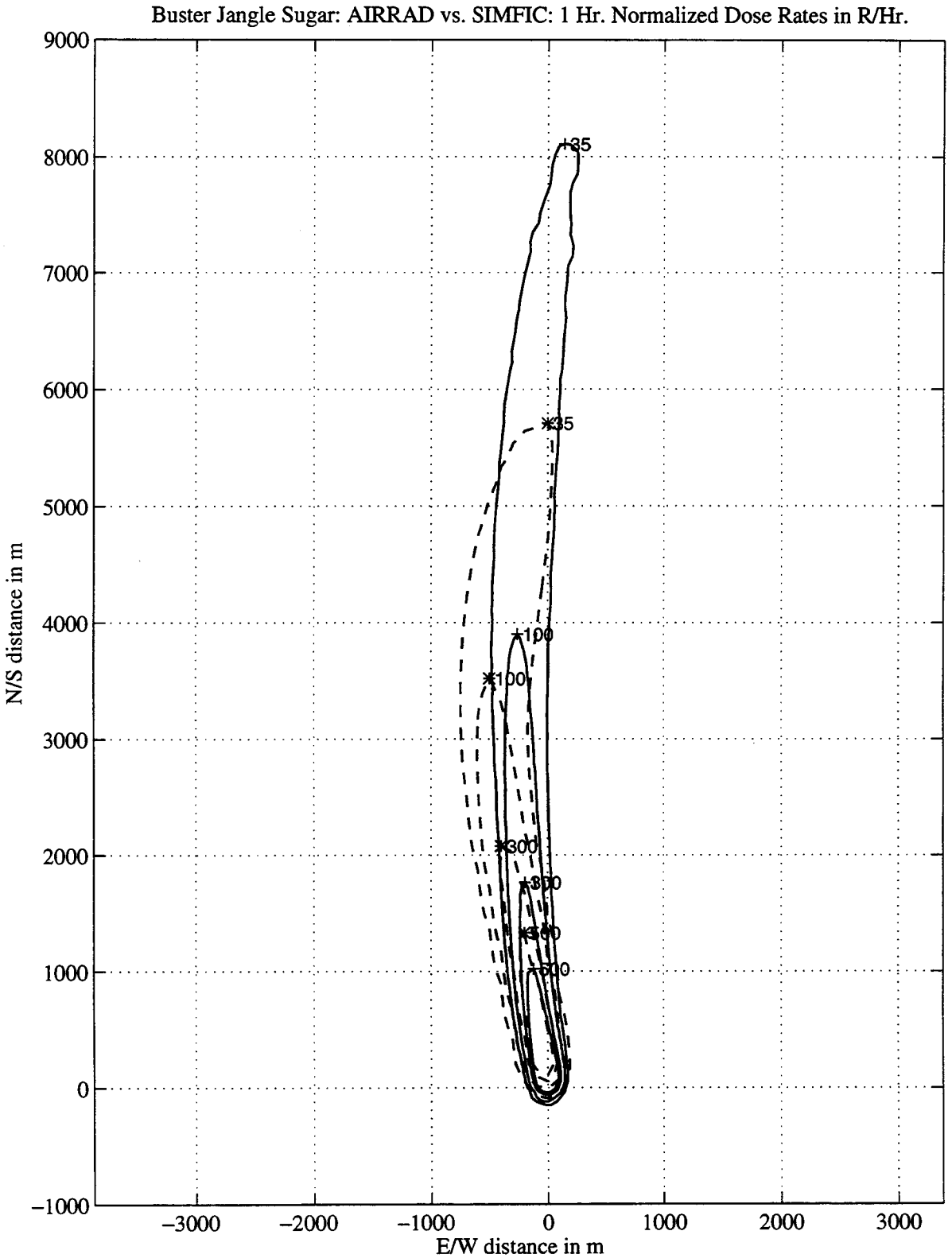

Figure 12: Buster Jangle Sugar full contours, AIRRAD (solid) vs. SIMFIC(dashed)

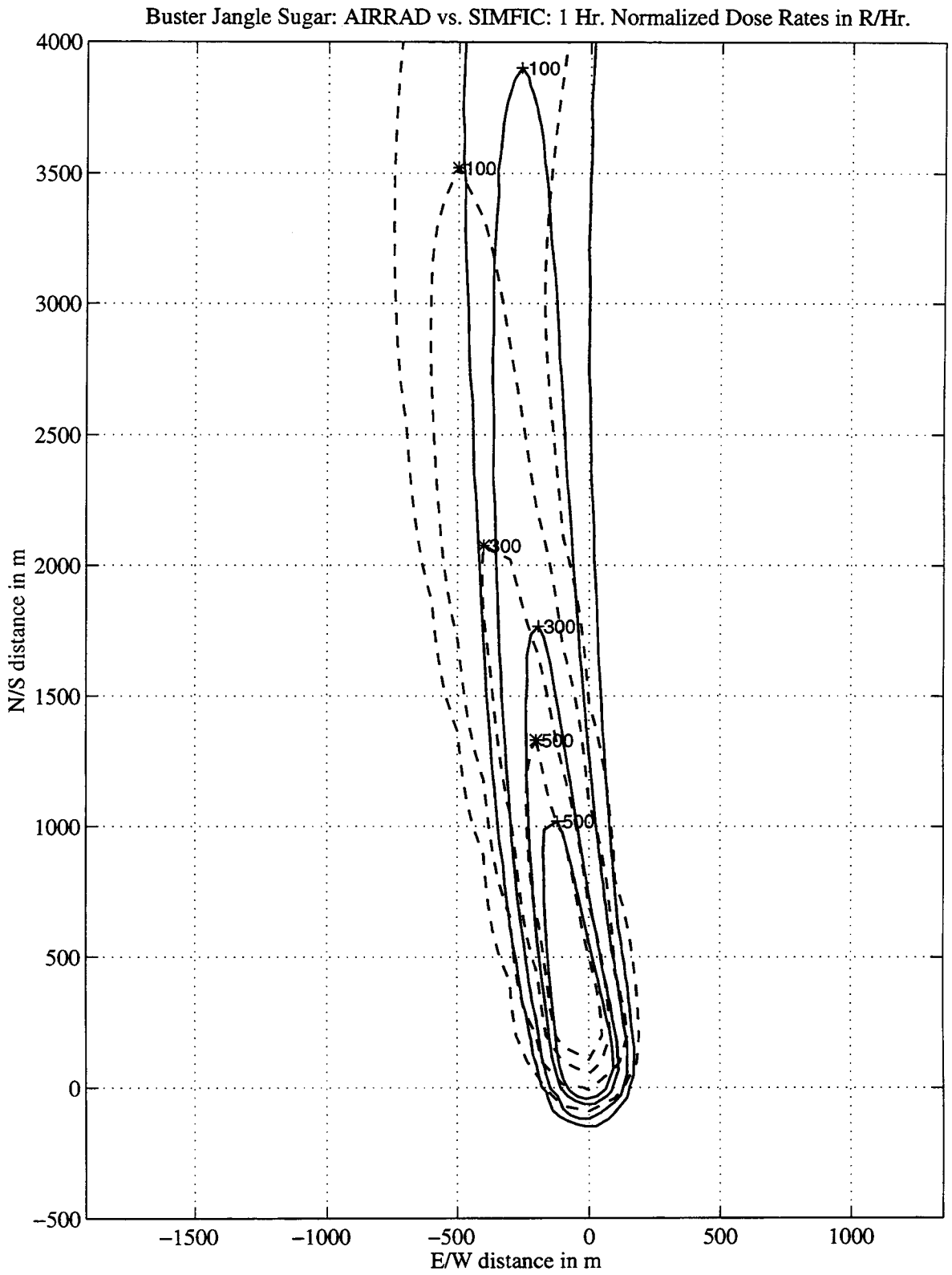

Figure 13: Buster Jangle Sugar partial contours, AIRRAD (solid) vs. SIMFIC (dashed)

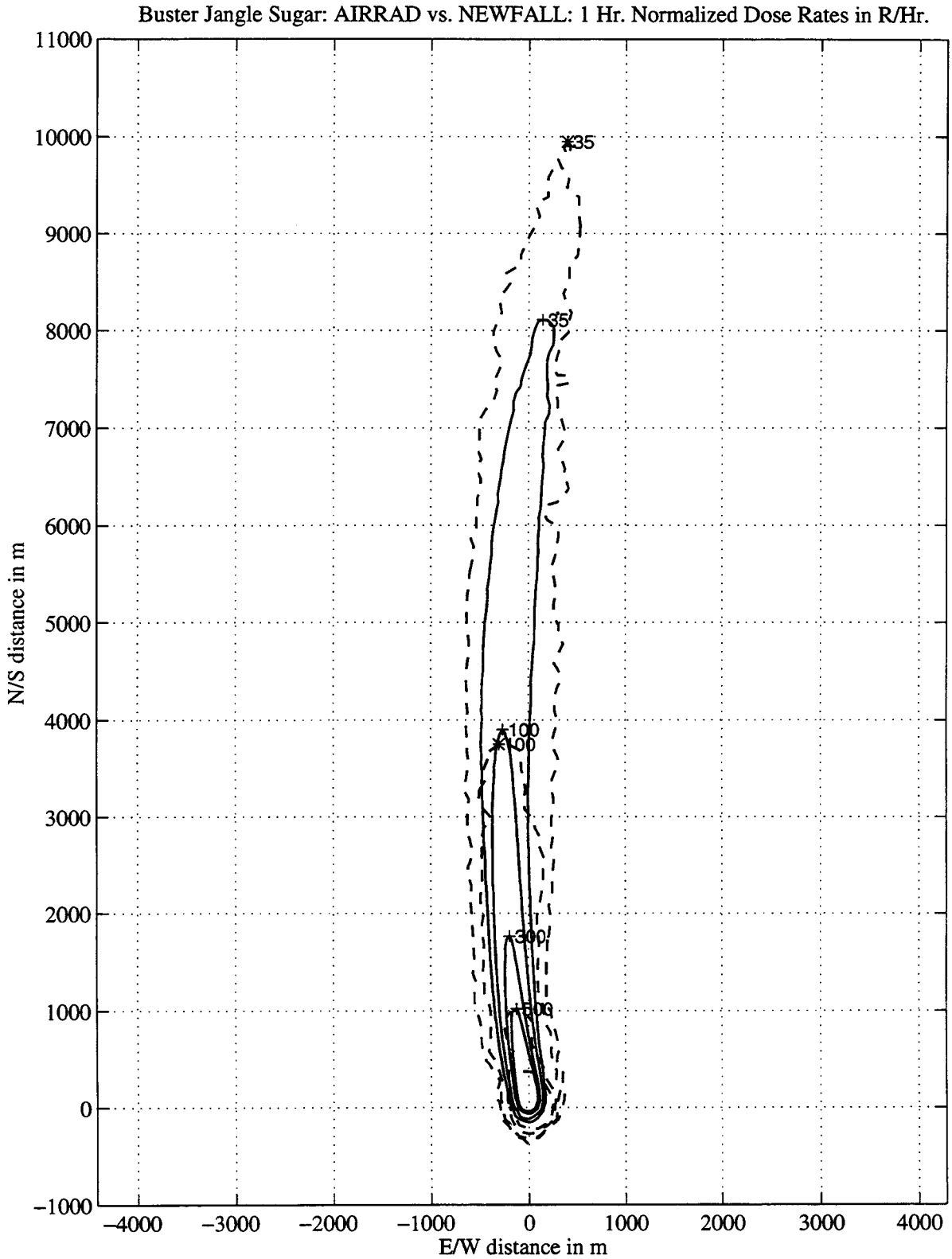

Figure 14: Buster Jangle Sugar contours, AIRRAD (solid) vs. NEWFALL (dashed)

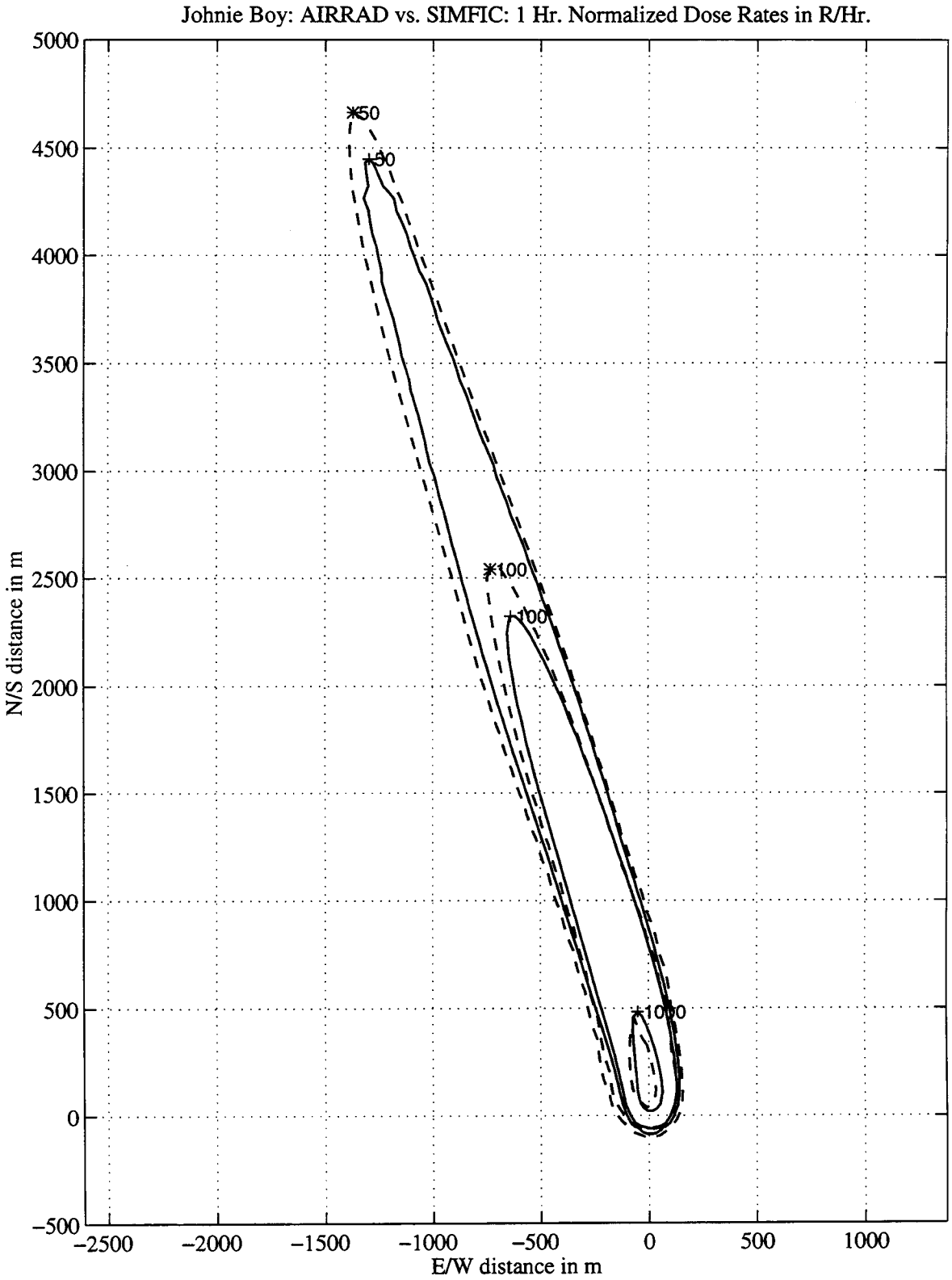

Figure 15: Johnnie Boy contours, AIRRAD (solid) vs. SIMFIC (dashed)

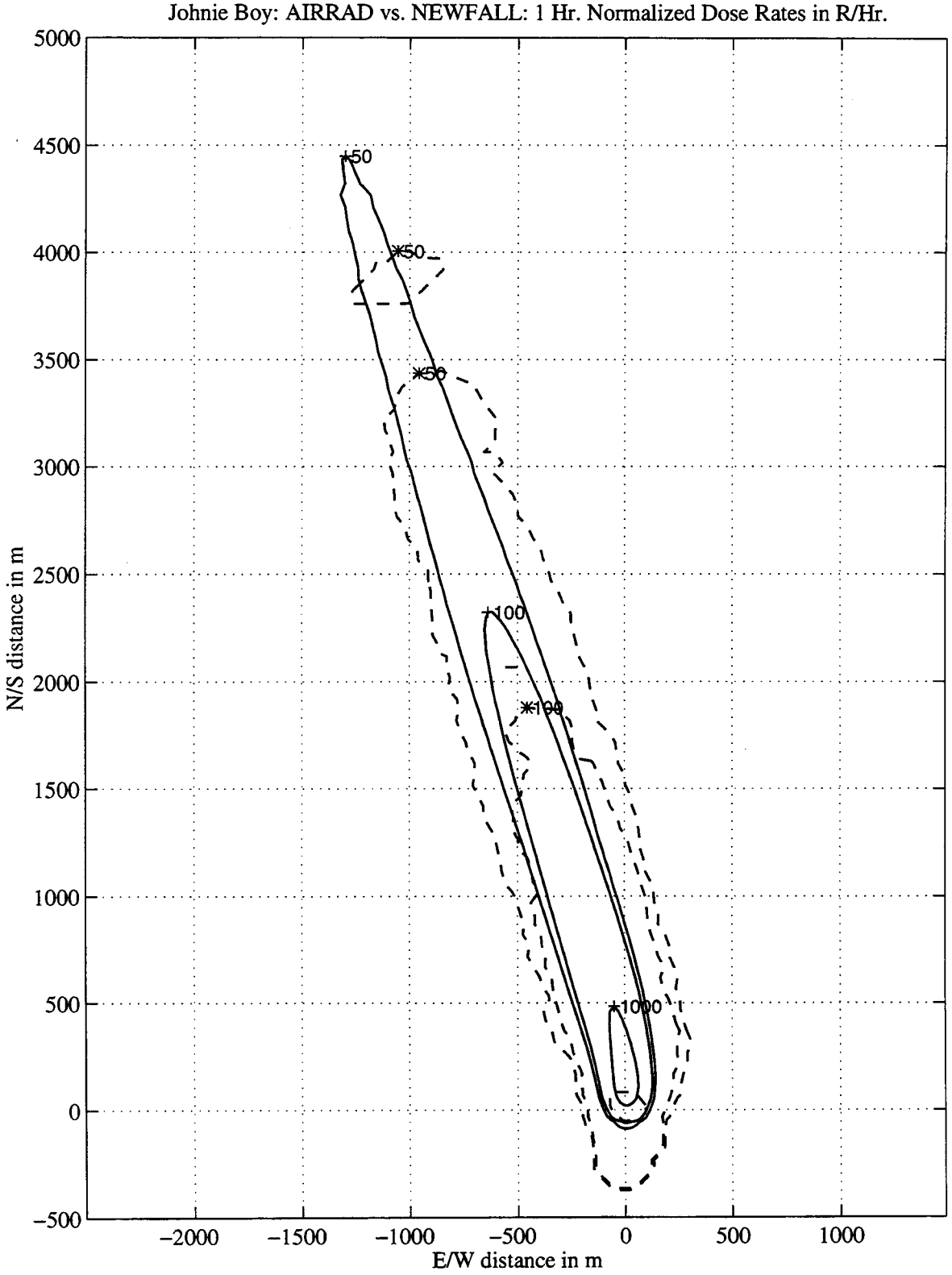

Figure 16: Johnnie Boy contours, AIRRAD (solid) vs. NEWFALL (dashed)

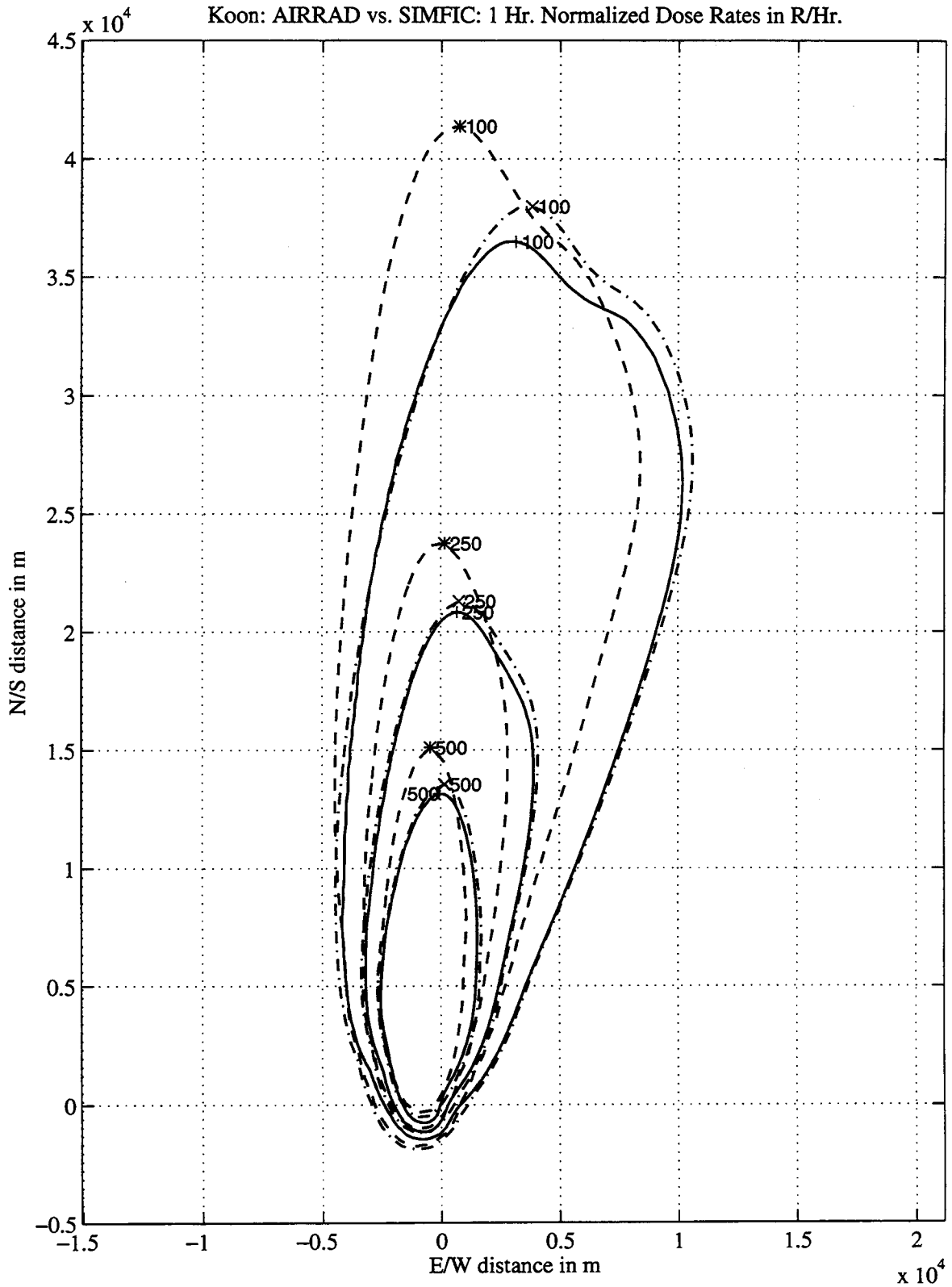

Figure 17: Koon contours, AIRRAD (solid) vs. SIMFIC (dashed) vs. modified SIMFIC (dot–dashed)

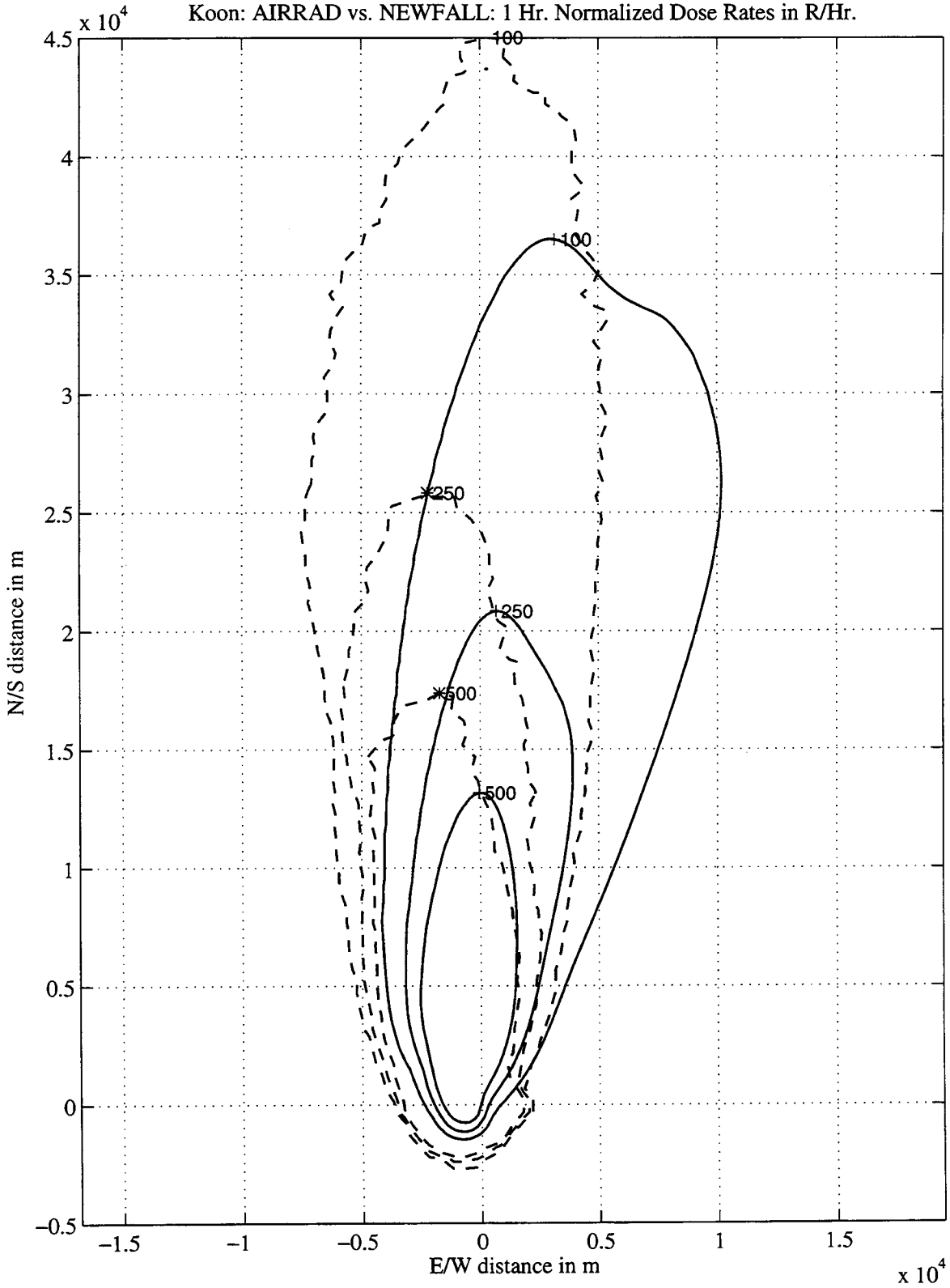

Figure 18: Koon contours, AIRRAD (solid) vs. NEWFALL (dashed)

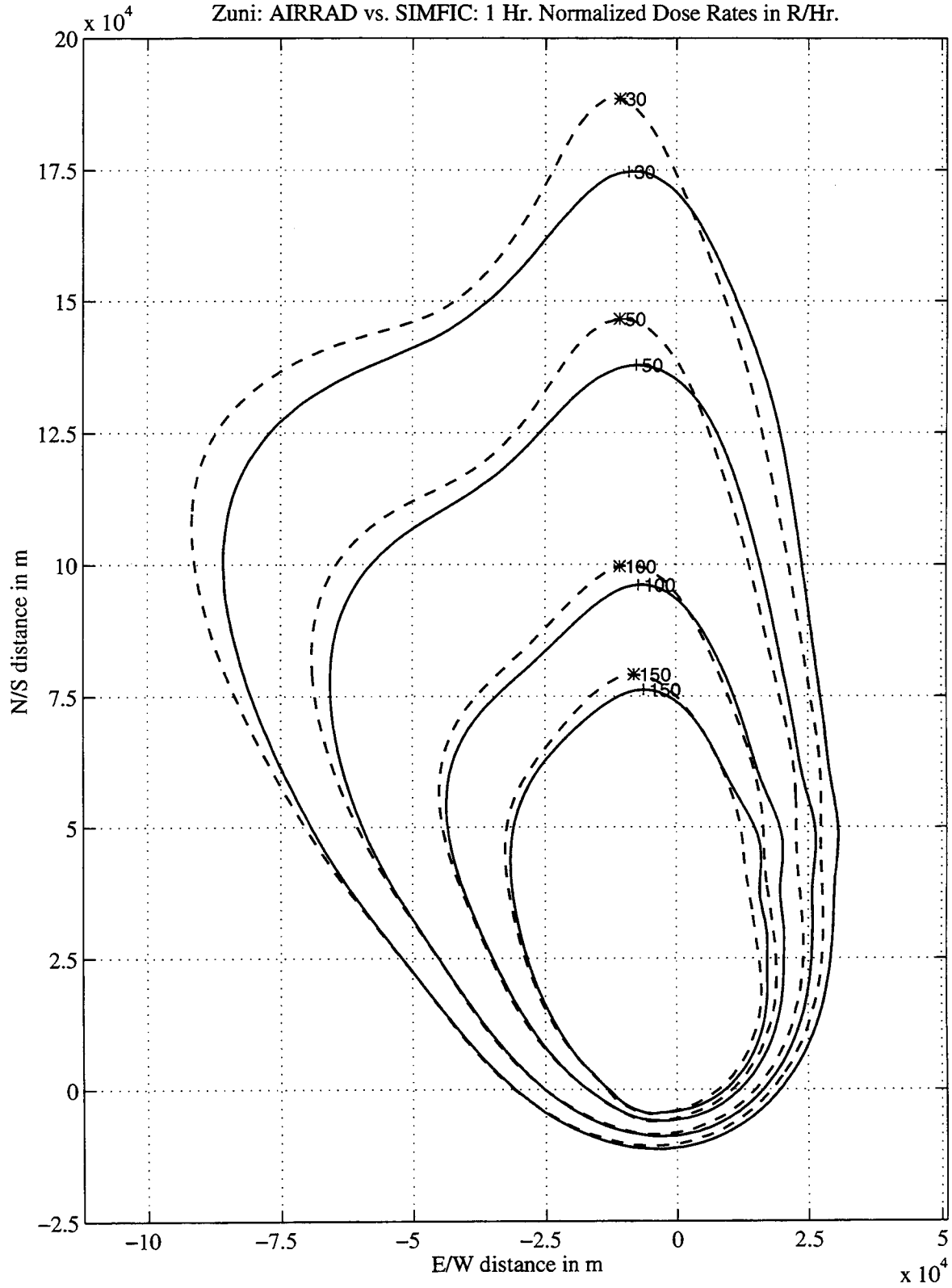

Figure 19: Zuni contours, AIRRAD (solid) vs. SIMFIC (dashed)

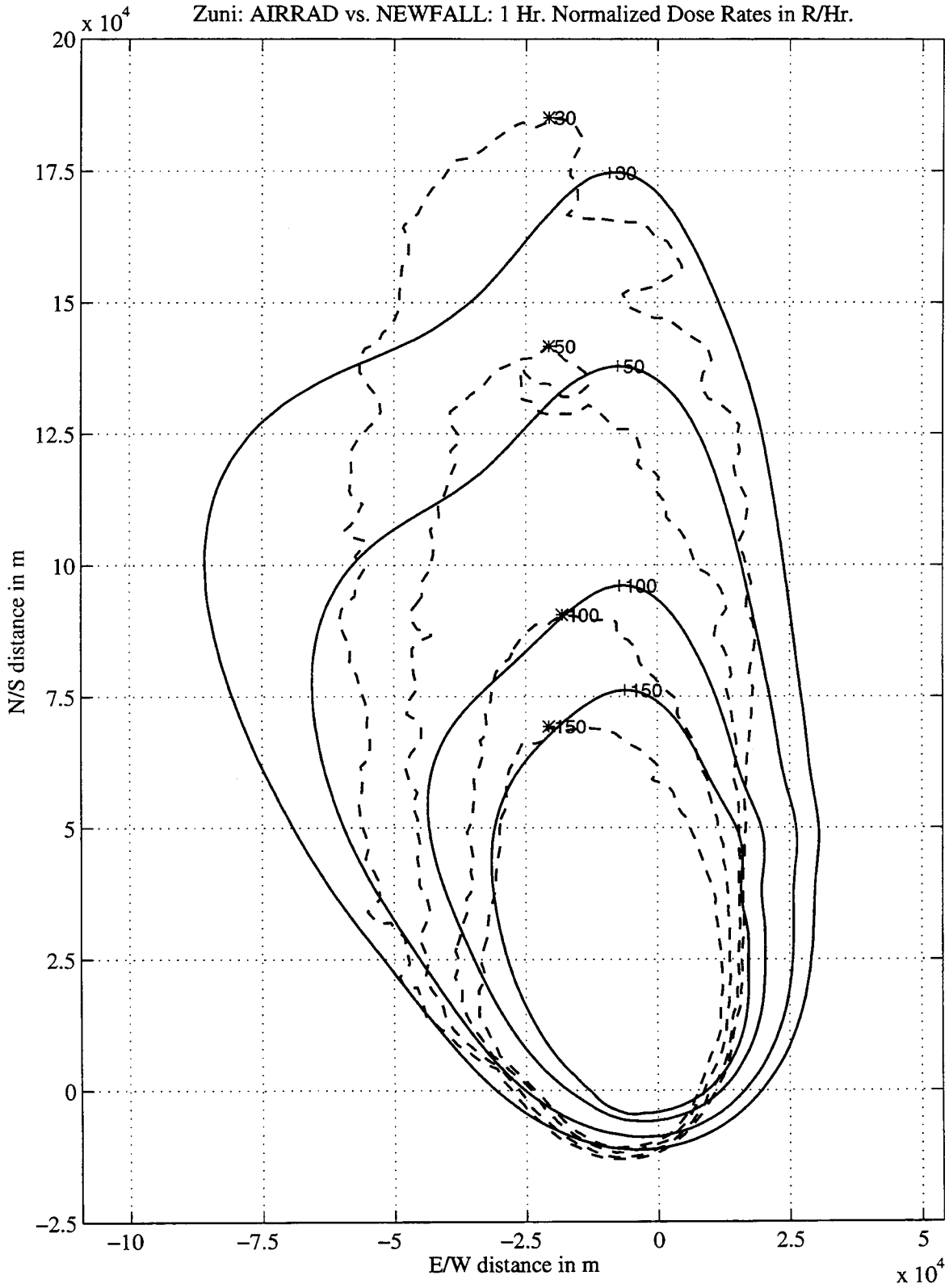

Figure 20: Zuni contours, AIRRAD (solid) vs. NEWFALL (dashed)

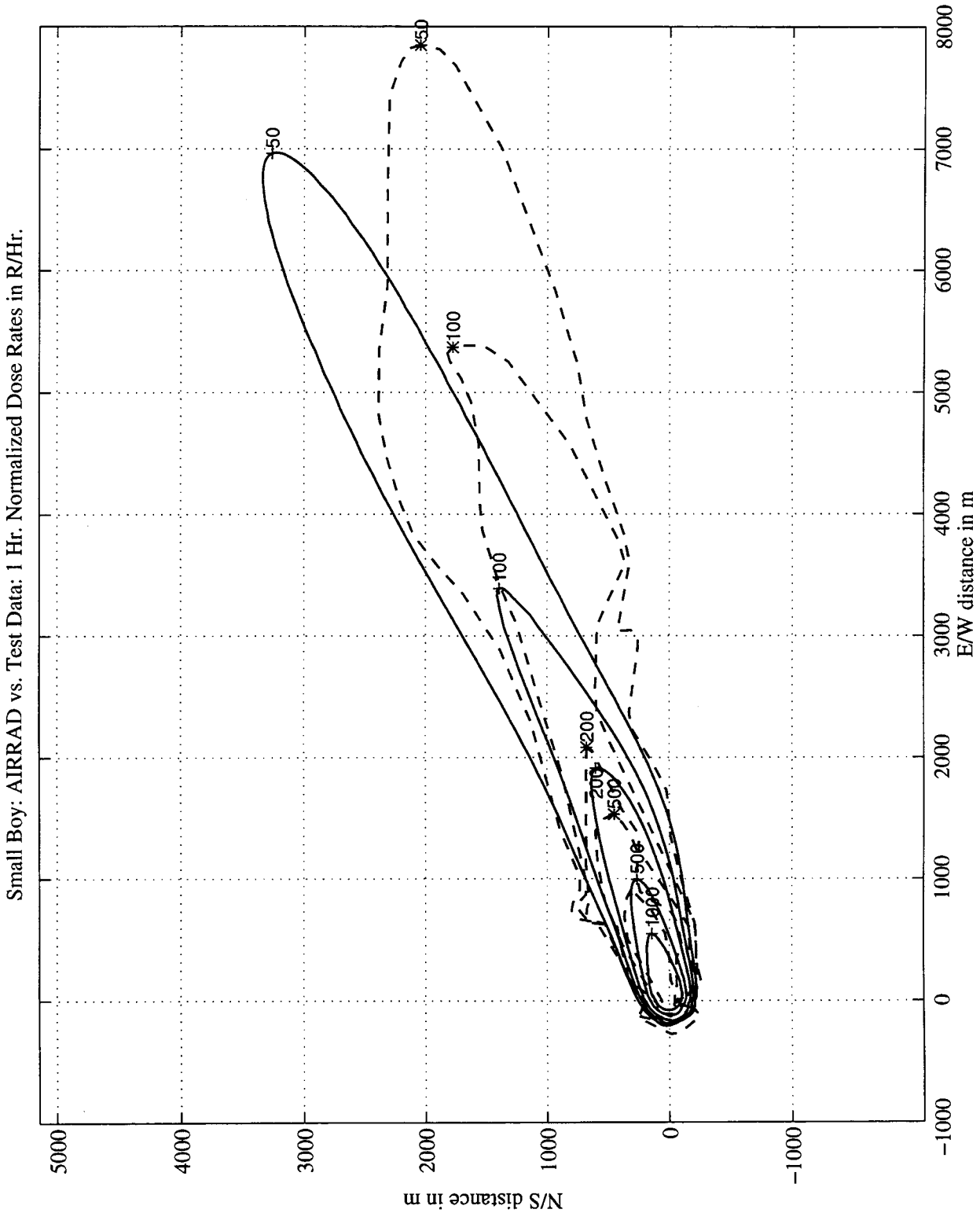

Figure 21: Small Boy contours, AIRRAD (solid) vs. Test Data (dashed)

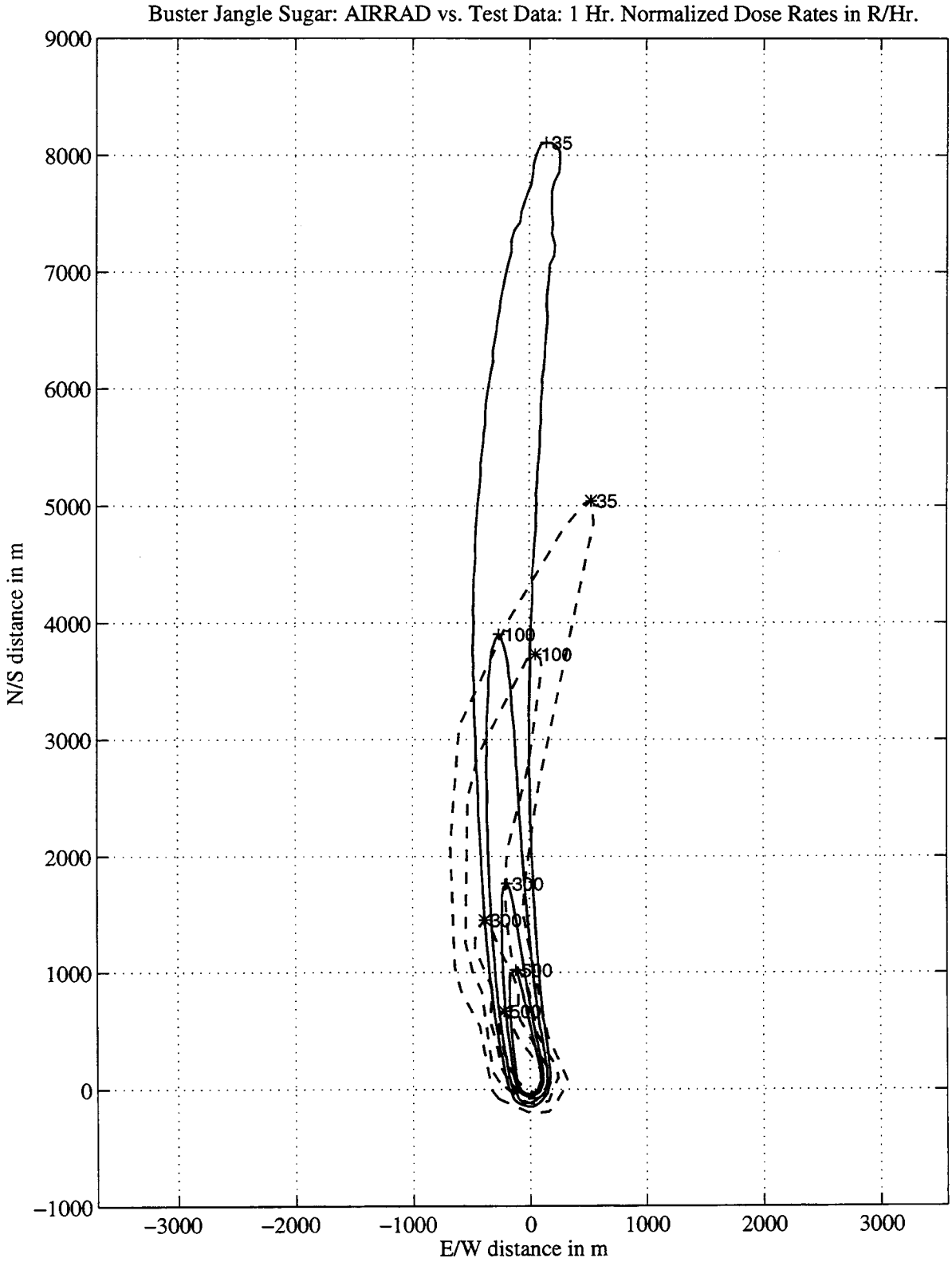

Figure 22: Buster Jangle Sugar contours, AIRRAD (solid) vs. Test Data (dashed)

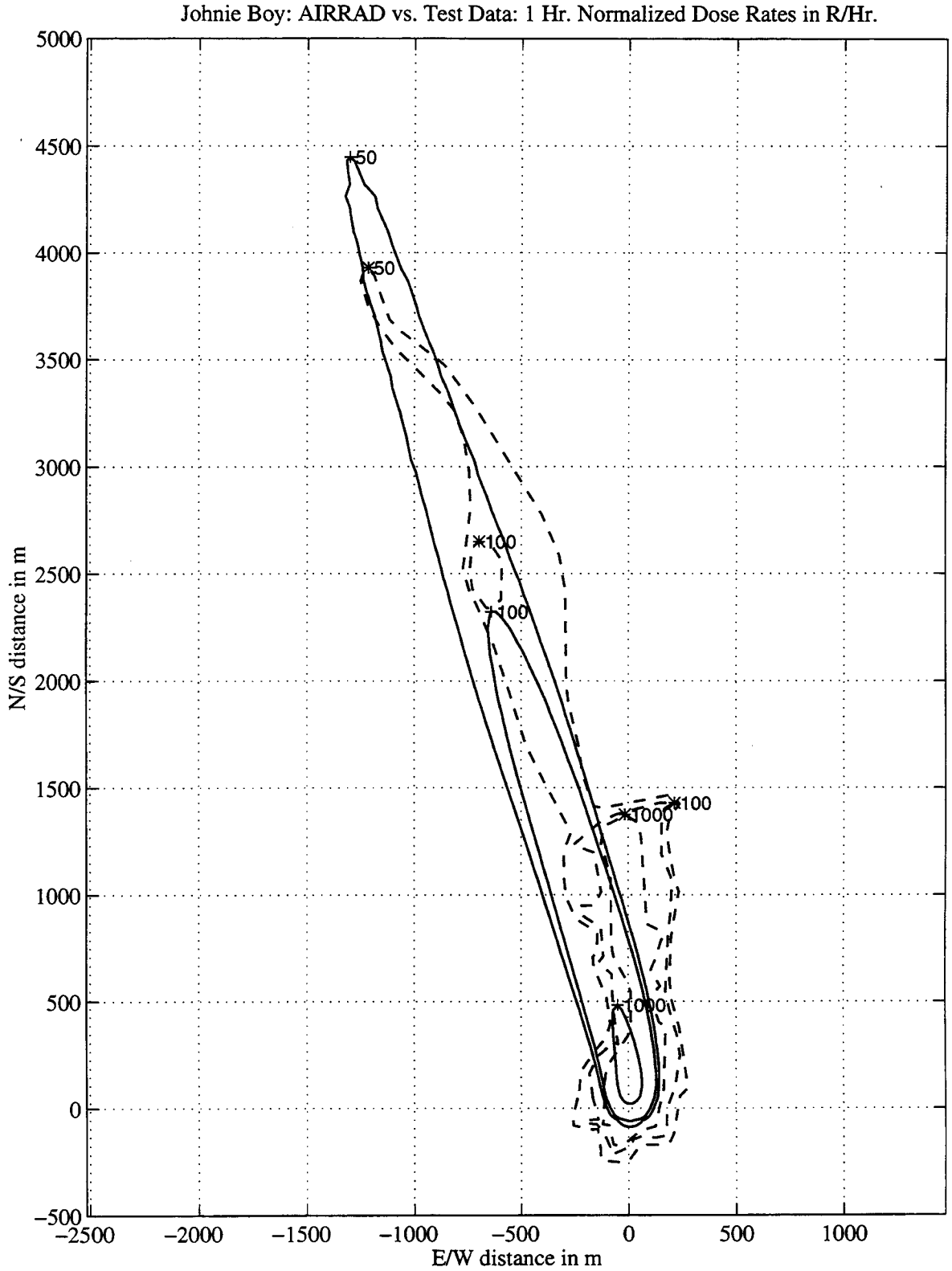

Figure 23: Johnie Boy contours, AIRRAD (solid) vs. Test Data (dashed)

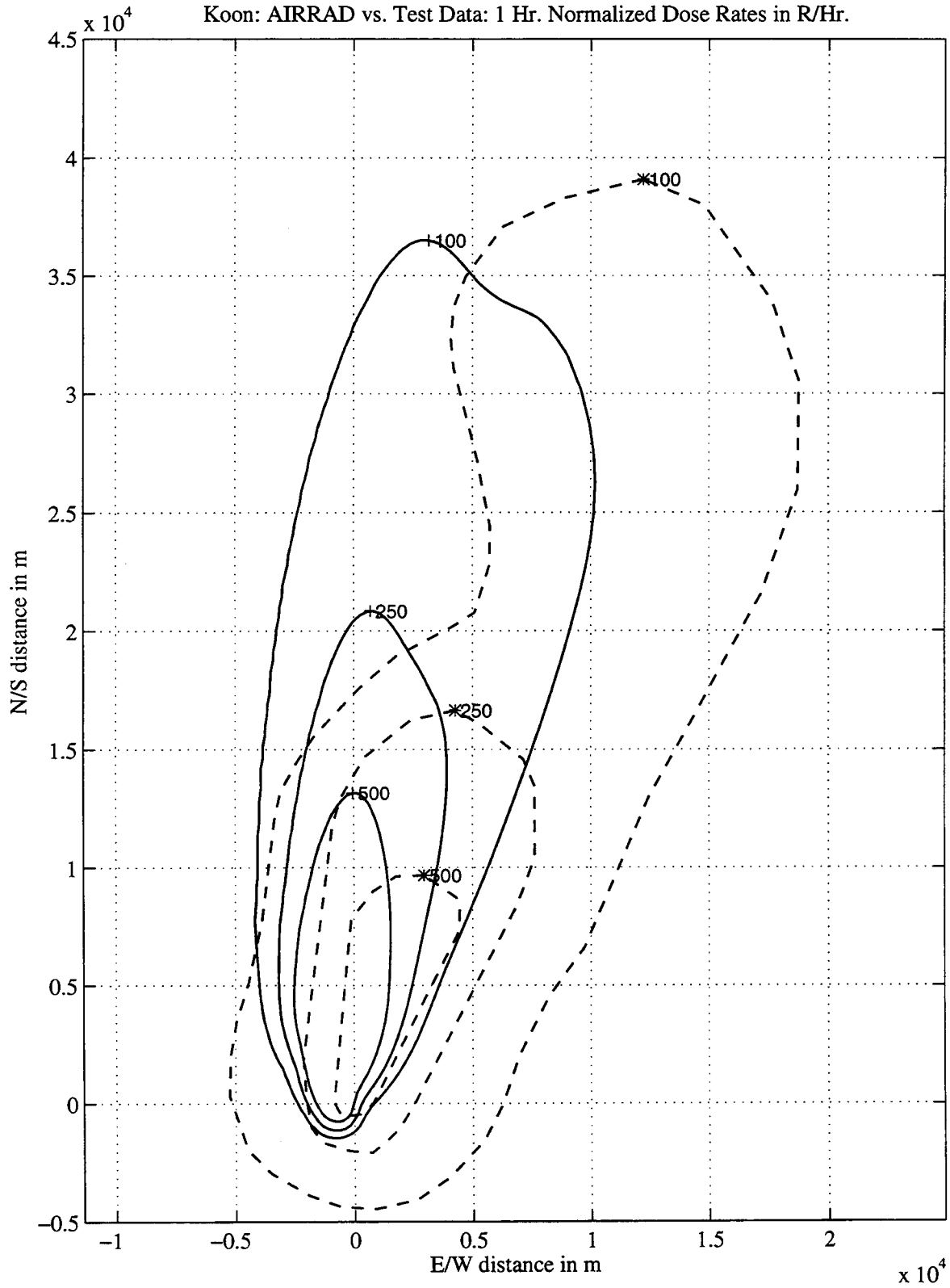

Figure 24: Koon contours, AIRRAD (solid) vs. Test Data (dashed)

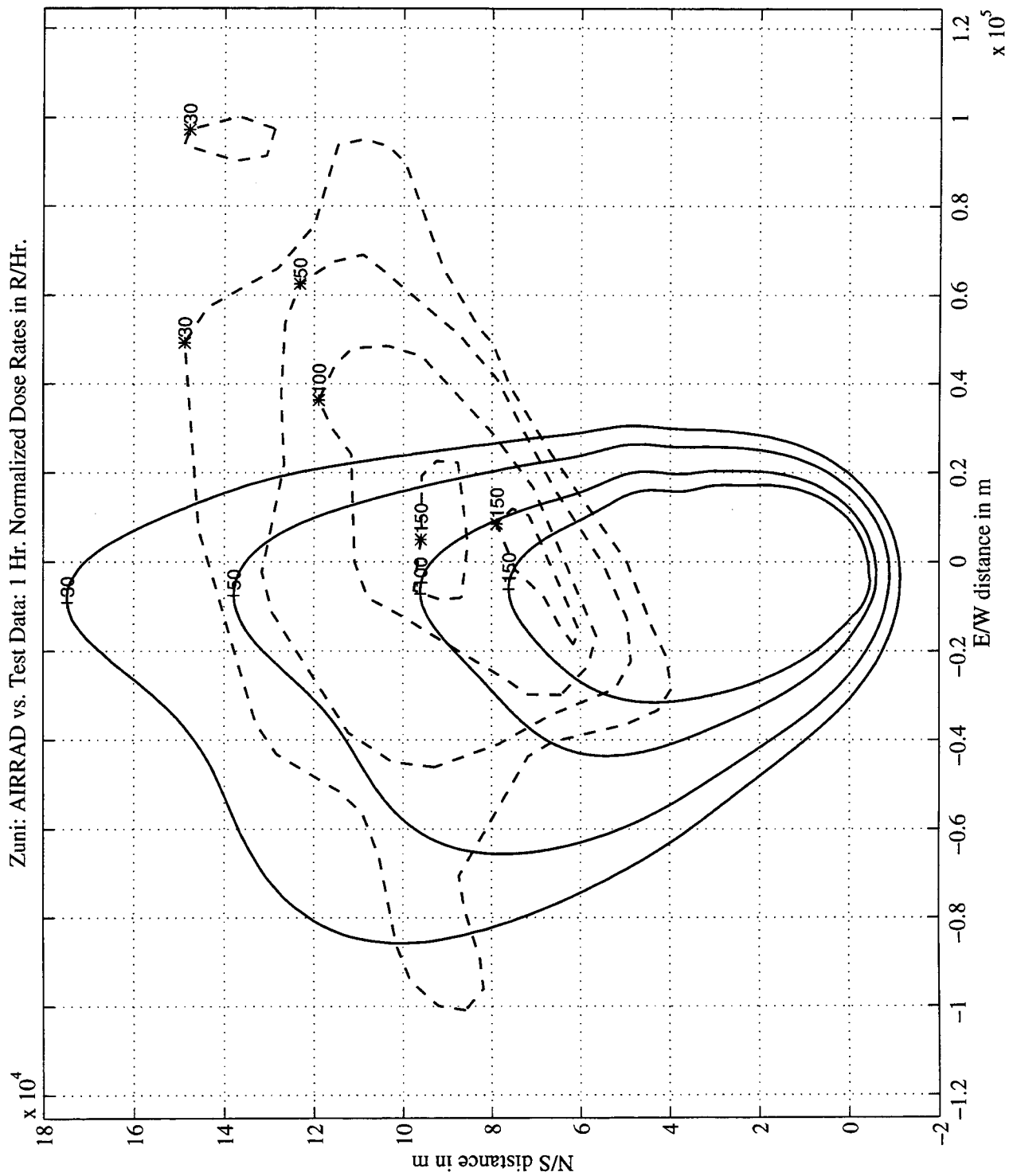

Figure 25: Zuni contours, AIRRAD (solid) vs. Test Data (dashed)

6 References

References

[1] H. G. Norment, "SIMFIC: A Simple, Efficient Fallout Prediction Model," DNA 5193F, December 31, 1979.

[2] H. G. Norment, "DELFIC: Department of Defense Fallout Prediction System, Volumes I and II," Atmospheric Science Associates, DNA 5159-1,2, October 26, 1979.

[3] H. G. Norment, "Evaluation of Three Fallout Prediction Models, DELFIC, SEER and WSEG-10 (U)," DNA 5285F, June 16, 1978. (SECRET)

[4] M. Morgenthau, et al., "Local Fallout from Nuclear Test Detonations, Volume II Compilation of Fallout Patterns and Related Test Data," NDL-TR-34/DASA-1251 Vol. II, parts 1-2, Nuclear Defense Laboratory, Edgewood Arsenal, Maryland, August 1963. (SECRET)

[5] R. L. Showers, et al., "Local Fallout from Nuclear Test Detonations, Volume II Compilation of Fallout Patterns and Related Test Data,", NDL-TR-34/DASA-1251 Vol. II, part3, Nuclear Defense Laboratory, Edgewood Arsenal, Maryland, March 1966. (SECRET)

[6] F. L. Wasmer, "Airrad Fallout Prediction System, Technical Report," Report to Sponsoring agencies, Sandia National Laboratories, Albuquerque NM and U.S. Army Atmospheric Sciences Laboratory White Sands Missile Range, NM, January, 1989.

[7] A. C. Best, "Empirical Formulae for the Terminal Velocity of Water Drops Falling Through the Atmosphere," Quarterly J. Royal Meteorological Society, Vol 76, 1950

[8] E. M. Wilkins, "Decay Rates for Turbulent Energy Throughout the Atmosphere," J. Atmospheric Sciences, Vol. 20 p. 473, 1963.

A The Original Simfic Report

Because Reference 1 is not widely distributed it was decided to include a complete and detailed description of the SIMFIC model. Much of this appendix is taken verbatim from Reference 1 but at the authors discretion, additional explanatory text has been added. Also, some nonessential text and information related only to the model implementation rather than the model itself, has been omitted. For consistency, the original equation numbering in Norment's report has been retained. The numbering scheme appends letters to some of his equation numbers to indicate that the relation is specific to a part of the cloud cap. Upper case B and T identify relations specific to the base and the top of the cloud cap, respectively. A lower case n is used for equations that involve nondimensional time or altitude variables.

Before becoming submerged in the details of the SIMFIC model, a short overview is given here to provide a frame of reference for the reader. The problem that is being solved is to calculate the down range distribution of radioactive debris from a nuclear detonation. The debris that can be transported significant distances is in the form of fairly small particulate that can remain airborne for a long time. The SIMFIC model deals only with particulate in a size range from 50 microns to 0.5 cm, and assumes that these particles are responsible for the majority of the radioactive fallout. Initially, the spatial distribution of particles is assumed to be uniform throughout the debris cloud and as the debris cloud rises, the particles rise with it. Eventually, the updraft of the rising cloud is dissipated and the particles settle back to earth. While the particles are in the air they are transported downrange by the ambient winds.

The model makes the simplifying assumption that, for purposes of calculating down range transport, particles rise to their maximum height according to a $\sqrt{t}$ power law. After reaching their maximum altitude the particles settle back to earth at their normal settling speed. If both the ambient wind speed as a function of altitude and the altitude vs time history of a particle are known, the particle down range transport can be computed. A simple integration over time of the wind speed at the particle location gives the downrange impact location. The key to calculating fallout is to be able to calculate the maximum altitude and time at which that altitude is reached for the fallout particles. If those quantities are known, the altitude vs time on the ascent is determined by the $\sqrt{t}$ power law and on the descent by the settling speed.

To keep the number of calculations within reason, SIMFIC treats the fallout as a series of concentric cylinders as described earlier in the text of the report. For each particle size class, transport calculations are actually done only for the six particles (assuming the cloud is modeled by five cylinders) at the middle of the bounding surfaces of the cylinders. The difficult part of the calculation is determining the altitude and time when each particle reaches it's apogee. To simplify these calculations, they are done in detail only for the bottommost and topmost of the six particles. An interpolation formula is used to estimate values for the remaining four particles. As the cylinders are transported down range they increase in size and the eventual fallout distribution on the ground from each cylinder is given in terms of a bivariate Gaussian distribution.

It is worth noting that the particle rise behavior is treated differently when doing calculations for the time and altitude at apogee than when doing transport calculations. In the apogee calculations, the cloud rise is assumed to follow a $\sqrt{t}$ power law, but the vertical speed of the particles differs from that of the cloud by their settling speed. For transport calculations, the particles are assumed to follow a strict $\sqrt{t}$ power law as they rise. If a particle reaches its peak altitude before the cloud stabilizes (quits rising), the effect of the updraft on the particle settling speed is ignored.

The SIMFIC model depends heavily on empirical relations to define many of its required parameters. Many of these relations were derived to conform to the DELFIC model, Reference 2, or to match results from test data. In the process of preparing this appendix and studying the contents of Norment's original report, some errors (often typos) were noted and are corrected here. Specifically, the following equations differ from the original report; (2.2.3), (2.2.11), (2.6.3), (2.6.4) and (2.9.3).

A.1 Vertical Trajectory Equations

In accord with the proportionality of cloud altitude with the square root of time, the altitudes of the base and top of the cloud cap, z_B and z_T, at time t are given by linear interpolation on $\sqrt{t}$ between initial and final altitudes, $z_{B,i}$, $z_{T,i}$, and $z_{B,s}$, $z_{T,s}$, as

$$z_B = z_{B,i} + \frac{\sqrt{t} - \sqrt{t_i}}{\sqrt{t_s} - \sqrt{t_i}}(z_{B,s} - z_{B,i}) \qquad (2.2.1B)$$

$$z_T = z_{T,i} + \frac{\sqrt{t} - \sqrt{t_i}}{\sqrt{t_s} - \sqrt{t_i}}(z_{T,s} - z_{T,i}) \qquad (2.2.1T)$$

where the cloud rise is taken to begin at time t_i after detonation and end at time t_s. Differentiation of Equations (2.2.1B and 2.2.1T) give the base and top velocities

$$u_B = \frac{z_{B,s} - z_{B,i}}{2\sqrt{t}(\sqrt{t_s} - \sqrt{t_i})} \qquad (2.2.2B)$$

$$u_T = \frac{z_{T,s} - z_{T,i}}{2\sqrt{t}(\sqrt{t_s} - \sqrt{t_i})} \qquad (2.2.2T)$$

Following DELFIC [2] we assume a linear variation of rise speed inside the cloud between z_B and z_T. Thus the vertical velocity of an in-cloud particle at altitude z with settling speed f is

$$\frac{dz}{dt} = u_B + (z - z_B)(u_T - u_B)/(z_T - z_B) - f; \quad z > z_B, \quad t < t_s \qquad (2.2.3)$$

The upward drift velocity of air below the cloud decreases linearly with distance from the cloud base, which gives for the below-cloud particle velocity

$$\frac{dz}{dt} = \frac{z}{z_B} u_B - f; \quad z \leq z_B, \quad t < t_s. \qquad (2.2.4)$$

At this point it is expedient to nondimensionalize the variables as follows:

$$\zeta = z/(z_{B,s} - z_{B,i}) \qquad (2.2.5)$$

$$\tau = \sqrt{t}/(\sqrt{t_s} - \sqrt{t_i}) \qquad (2.2.6)$$

$$v = \frac{d\zeta}{d\tau} = 2\tau u(\sqrt{t_s} - \sqrt{t_i}), \qquad (2.2.7)$$

As a physical reference, $\zeta = 1$ is the dimensionless distance that the cloud base rises from initial time to stabilization. Also, $\tau = 1$ represents the increment of time from the initial cloud formation time to cloud stabilization. A nondimensional, average settling speed (defined later) is

$$\hat{f} =< f > (\sqrt{t_s} - \sqrt{t_i})^2/(z_{B,s} - z_{B,i}). \qquad (2.2.8)$$

In dimensionless form Equations (2.2.1) and (2.2.2) become

$$\zeta_B = \zeta_{B,i} + \tau - \tau_i \qquad (2.2.1Bn)$$

$$\zeta_T = \zeta_{T,i} + (\tau - \tau_i)(\zeta_{T,s} - \zeta_{T,i}) \qquad (2.2.1Tn)$$

$$v_B = 1 \qquad (2.2.2Bn)$$

$$v_T = \zeta_{T,s} - \zeta_{T,i} \qquad (2.2.2Tn)$$

For an in-cloud particle we have

$$v = 1 + \frac{\zeta - \zeta_{B,i} - \tau + \tau_i}{\tau - \tau_i + a} - 2\tau\hat{f}\ ; \quad \zeta > \zeta_B, \quad \tau < \tau_s \quad (2.2.3n)$$

where

$$a = \frac{\zeta_{T,i} - \zeta_{B,i}}{\zeta_{T,s} - \zeta_{T,i} - 1} \qquad (2.2.9)$$

and for the below-cloud particle we have

$$v = \frac{\zeta}{\tau - \tau_i + \zeta_{B,i}} - 2\tau\hat{f}\ ; \quad \zeta \leq \zeta_B\ , \quad \tau < \tau_s. \quad (2.2.4n)$$

After the cloud stops rising we have

$$v = -2\tau\hat{f}\ ;\quad \tau > \tau_s. \qquad (2.2.10)$$

Equations (2.2.3n), (2.2.4n) and (2.2.10) can be integrated to give the vertical trajectory equations for particles in the cloud cap and for particles below the cloud cap. The vertical trajectory of a particle that started out at location ζ_i is:
In-cloud

$$\zeta - \zeta_i = (a + \zeta_i - \zeta_{B,i})\frac{\tau - \tau_i}{a} - 2\hat{f}(\tau - \tau_i + a) \times$$

$$\left[\tau - \tau_i + (\tau_i - a)\ln\left(\frac{\tau - \tau_i + a}{a}\right)\right];\quad \zeta > \zeta_B,\ \ \tau < \tau_o,\ \ \tau < \tau_s \qquad (2.2.11)$$

Below-cloud

$$\zeta - \zeta_o = \zeta_o\frac{\tau - \tau_o}{\tau_o - \tau_i + \zeta_{B,i}} - 2\hat{f}(\tau - \tau_i + \zeta_{B,i}) \times$$

$$\left[\tau - \tau_o + (\tau_i - \zeta_{B,i})\ln\left(\frac{\tau - \tau_i + \zeta_{B,i}}{\tau_o - \tau_i + \zeta_{B,i}}\right)\right];\quad \zeta \le \zeta_B,\ \ \tau_o < \tau < \tau_s \qquad (2.2.12)$$

After completion of the cloud rise

$$\zeta = \zeta_{\tau=\tau_s} - \hat{f}(\tau^2 - \tau_s^2);\quad \tau > \tau_s\ . \qquad (2.2.13)$$

where τ_o and ζ_o are the nondimensional time and altitude at which the particle drops out of the cloud cap, i.e. drops below ζ_B. Variable ranges included in the above equations serve as a reminder that (2.2.11) is valid only prior to stabilization and while the particle is in the cloud and (2.2.12) is valid only prior to stabilization and while the particle is beneath the cloud cap. Equation (2.2.13) gives the particle elevation after completion of the cloud rise.

A.2 Time and Altitude of Particle Separation from the Cloud

For the above equations to be useful, we must be able to calculate τ_o and ζ_o. A particle falls out of the cloud cap when $\zeta = \zeta_B$. By substituting Equation (2.2.1B) into the left side of Equation (2.2.11) and some algebraic manipulation we obtain

$$\tau_o - \tau_i + a + (\tau_i - a)\ln(\tau_o - \tau_i + a) = \frac{\zeta_i - \zeta_{B,i}}{2a\hat{f}}$$

$$+(\tau_i - a)\ln(a) + a. \qquad (2.3.1)$$

which can be written in a simple shorthand form

$$\xi + b\ln\xi = c \qquad (2.3.2)$$

For a given particle initial location ζ_i and known device detonation parameters (as described later) all of the terms in Equation (2.3.1) are know except τ_o. Thus we have a transcendental equation for τ_o, which can be solved using iterative techniques. Once the value of τ_o is known it can be substituted into Equation (2.2.11) to determine ζ_o.

A.3 Maximum Particle Height

The quantities that are actually used in fallout prediction calculations are the maximum altitude and time this altitude is reached, along with a profile of wind speed vs altitude. For in-cloud particles, setting the vertical dimensionless velocity in Equation (2.2.3n) to 0 yields an expression for the peak altitude, ζ_m in terms of the time that this altitude occurs, τ_m.

$$\zeta_m = \zeta_{B,i} - a + 2\tau_m \hat{f}(\tau_m - \tau_i + a) \qquad (2.4.1)$$

Substituting this relation into Equation (2.2.11) and performing some simplifying algebraic manipulations gives an equation of the same form as (2.3.2), but for which

$$\xi = \tau_m - \tau_i + a$$

$$b = (\tau_i - a)/2$$

$$c = \frac{a + \zeta_i - \zeta_{B,i}}{4\hat{f}a} + b\ln(a) + \tau_i/2 + a.$$

As with Equation (2.3.2) Newton iteration is used to solve for ξ, τ_m is recovered from ξ, and ζ_m is found by substitution of τ_m into Equation (2.4.1).

For below-cloud particles, the left side of Equation (2.2.4n) is set to zero and solving for ζ_m in terms of τ_m gives,

$$\zeta_m = 2\tau_m \hat{f}(\tau_m - \tau_i + \zeta_{B,i}) \qquad (2.4.2)$$

Substituting this expression into Equation (2.2.12), and after algebraic manipulation we again arrive at an equation of the same form as Equation (2.3.2), but with

$$\xi = \tau_m - \tau_i + \zeta_{B,i}$$

$$b = (\tau_i - \zeta_{B,i})/2$$

$$c = \frac{\zeta_o}{4\hat{f}(\tau_o - \tau_i + \zeta_{B,i})} + \tau_0/2 + b\ln(\tau_o - \tau_i + \zeta_{B,i}) - \tau_i + \zeta_{B,i}.$$

As before, this is solved for ξ by Newton iteration, etc.

Because multiple equations, each with a limited range of applicability, are used to solve for τ_m and ζ_m, various possibilities must be examined when performing the calculations. Reference 1 gives a set of four cases in a very cryptic form along with instructions for which equations to use. Here the author's attempt at a more easily understandable explanation is given first and then the exact quote is presented.

For particles that are still within the cloud at stabilization time, i.e., $\tau_o > \tau_s$, only the in-cloud equations should be used. If the time at maximum altitude, τ_m, predicted by these equations occurs before stabilization time, i.e., $\tau_m < \tau_s$, then use the in-cloud predicted time and the corresponding maximum altitude for τ_m and ζ_m. However, since

the cloud is still rising at stabilization time[8], it can happen that some of the very fine particles are also still rising at stabilization time. In that case, the in-cloud equations predict $\tau_m > \tau_s$. Because the model is intended to cut off the cloud rise phase of the fallout process at stabilization time, use the stabilization time and altitude at stabilization time predicted by the in-cloud equations as τ_m and ζ_m.

For particles that drop out of the cloud before stabilization time, i.e., $\tau_o < \tau_s$, there are two possibilities. A particle may still be rising when it drops out of the cloud or it may be falling when it drops out of the cloud. For particles that are still rising at τ_o, the below-cloud equations must be used. As long as the τ_m predicted by the below-cloud equations occurs before τ_s, use τ_m and ζ_m as predicted by the below-cloud equations. However, if the calculated $\tau_m > \tau_s$, use the stabilization time and altitude at stabilization time predicted by the below-cloud equations for τ_m and ζ_m. In the case of a particle falling as it drops out of the cloud, τ_m and ζ_m calculated by the in-cloud equations are applicable and should be used. To test whether or not the particle is rising or falling as it drops out of the cloud, substitute the values for τ_o and ζ_o for τ and ζ into Equation (2.2.4n), which give the below cloud particle velocity. A negative value for ζ indicates the particle was falling when it dropped out of the cloud cap.

[Exact quote] To select appropriate values for τ_m and ζ_m various possibilities must be examined. (Subscripts ic and bc denote in-cloud and below-cloud):

1. If $\tau_o > \tau_s$ and $\tau_m|_{ic} > \tau_s$, then set $\tau_m = \tau_s$ and calculate ζ_m by substitution of τ_s into Equation (2.2.11).
2. If $\tau_o > \tau_s$ and $\tau_m|_{ic} \leq \tau_s$, then use $(\tau_m, \zeta_m)_{ic}$.
3. If $\tau_o \leq \tau_s$ and $\tau_s \geq \tau_m|_{bc} > \tau_o$ and $\zeta_m|_{bc} > \zeta_m|_{ic}$ or $\tau_m|_{ic} > \tau_o$ use $(\tau_m, \zeta_m)_{bc}$.
4. If $\tau_o \leq \tau_s$ and $\tau_m|_{bc} > \tau_o$ and $\zeta_m|_{bc} > \zeta_m|_{ic}$ or $\tau_m|_{ic} > \tau_o$, but $\tau_m|_{bc} > \tau_s$ then set $\tau_m = \tau_s$ and compute ζ_m by substitution of τ_s into Equation (2.2.12).

Since the computations for apogee time and altitude are quite complex, it is suggested that these values be calculated for particles that are initially at the top and at the bottom of the cloud cap. That simplifies the calculations dramatically because a particle at the base of the cloud cap immediately falls out and is usually governed by case 3. For particles that start out at intermediate positions in the cloud the interpolation formulas are:

$$t_m = t_{m_B} + k^{0.85}(t_{m_T} - t_{m_B}) \qquad (2.4.3)$$

and

$$z_m = z_{m_B} + k^{0.85}(z_{m_T} - z_{m_B}) \qquad (2.4.4)$$

where $k = (z_i - z_{B,k})/(z_{T,i} - z_{B,i})$, t_{m_B} and z_{m_B} are apogee time and altitude for a particle at the center of the bottom disk, and t_{m_T} and z_{m_T} are apogee time and altitude for a particle at the center of the top disk.

[8]This is an artifact of assuming a $\sqrt{t}$ behavior for the cloud rise. For $t > 0$ the $\sqrt{t}$ is monotonically increasing.

A.4 Advection and Settling

A single vertical profile of wind vectors is input to the model. The altitudes at which the vectors are defined are used to stratify the atmosphere vertically into wind layers, in each of which the wind vector is uniform. Advection and settling of fallout particles is separated into two phases: 1. Rise of the particle to its maximum height z_m at time t_m and 2. settlement of the particle from z_m to the ground. Thus if $\vec{X}$ is the position vector, relative to ground zero, of a ground impacted fallout particle we have

$$\vec{X} = \sum_{z=0}^{z_m} \vec{W}_z \triangle t|_{rise} + \sum_{z_m}^{0} \vec{W}_z \triangle z/f|_{settlement} \qquad (2.5.2)$$

where the summations are over the wind layers of depth $\triangle z$ between the ground ($z = 0$) and the particle maximum height z_m, $\triangle t$ is the time spent in a wind layer, and $\vec{W}_z$ is the wind vector at height z.

During the rise phase, the particle altitude varies roughly as the square root of time. Therefore the time a particle spends in the i'th wind layer, $\triangle t_i$, is approximately

$$\triangle t_i = t_m \triangle(z^2)_i / z_m^2 \qquad (2.5.2)$$

where $\triangle(z^2)_i = z_{b,i+1}^2 - z_{b,i}^2$, and $z_{b,i}$ is the height of the base of the i'th wind layer.

If we define an average settling speed between z_m and the ground, $< f >$, and substitute Equation (2.5.2) into (2.5.1) we obtain

$$\vec{X} = \frac{t_m}{z_m^2} \sum_{z=0}^{z_m} \vec{W}_z \triangle(z^2) + < f >^{-1} \sum_{z=0}^{z_m} \vec{W}_z \triangle z. \qquad (2.5.3)$$

To avoid repetitive calculations of the sums in Equation (2.5.3), they are precalculated from the ground to each wind layer and stored. The average particle settling speed is derived as follows. Best, [7], has devised the simple equation

$$f = f_o e^{bz} \qquad (2.5.4)$$

for water drops, where f_o is the settling speed at sea level, z is altitude (meters) and

$$b = 2.90x10^{-5}; \quad 50 < \delta < 300 \quad \mu m$$

$$b = 4.05x10^{-5}; \quad 300 < \delta < 6000 \quad \mu m$$

where δ is the water drop diameter. These relations also give adequate results for fallout particles.

The average settling speed between altitudes z_1 and z_2 is determined by integration of Equation (2.5.4) to give

$$< f >= f_o \frac{e^{bz_2} - e^{bz_1}}{b\,(z_2 - z_1)} \qquad (2.5.5)$$

A.5 Cloud Definition

Following DELFIC, the initial cloud is defined at a time close to the fireball second temperature maximum

$$t_i = 2.07\, W^{0.19}, \qquad t \text{ in s} \;\; W \text{ in } kT, \qquad (2.6.1)$$

with radius

$$R_i = 108\, W^{0.33}, \qquad R \text{ in m}, \qquad (2.6.2)$$

with base altitude

$$z_{B,i} = z_{gz} + z_{hob} + 90W^{1/3} - .66144R_i, \qquad z \text{ in m} \qquad (2.6.3)$$

and top altitude

$$z_{T,i} = z_{gz} + z_{hob} + 90W^{1/3} + .66144R_i, \qquad z \text{ in m} \qquad (2.6.4)$$

The subscripts gz and hob are used to designate ground zero (the burst location) and height of burst, respectively. Many of the empirical equations that follow are not dimensionally consistent, so the numerical values must be given in specific units unless otherwise noted: W must be in kT, distances and altitudes are in meters, and wind speeds are in m/s.

Stabilized cloud heights are

$$z_{B,s} = z_{gz} + z_{hob} + aW^b \qquad (2.6.5)$$

$$z_{T,s} = z_{gz} + z_{hob} + cW^d \qquad (2.6.6)$$

where

$$a = 2228,\ b = 0.3463;\ W \leq 4.07$$
$$a = 2661,\ b = 0.2198;\ W > 4.07$$
$$c = 3597,\ d = 0.2553;\ W \leq 2.29$$
$$c = 3170,\ d = 0.4077;\ 2.29 < W \leq 19$$
$$c = 6474,\ d = 0.1650;\ W > 19.$$

Stabilized cloud radius is computed from

$$R_s = \exp\left(6.7553 + 0.7381\, Y + 0.060308\, Y^2\right) \qquad (2.6.7)$$

where $Y = \log_{10}(W)$

Table 1
Cloud Stop and Stabilization Times

Yield (kT)	Stop Time (s)	Stabilization Time (s)
10^{-3}	300	421
10^{-2}	300	421
10^{-1}	300	381
1	300	382
10	300	422
10^{2}	280	663
10^{3}	200	783
10^{4}	160	787
10^{5}	150	991

[note: Norment does not define the stop time given in the above table and the author could not find it used anywhere in the model.] Stabilized cloud radius is computed from

$$R_s = \exp\left(6.7553 + 0.7381\,Y + 0.060308\,Y^2\right) \qquad (2.6.7)$$

where $Y = \log_{10}(W)$.

At the initial time the cloud cap is partitioned into a stack of cylinders as shown in Figure (1) in the main body of this report. The fallout particles are initially assumed to be uniformly distributed inside the cloud cap. Fallout particles are grouped into many different size classes and the model does a separate set of calculations for each size class in each cylinder. Fallout particles of one size class in one cylinder are referred to by Norment as parcels and the bounding disks are referred to as wafers.

To keep track of a parcel, the model does trajectory calculations for the individual particles at the center of the upper and lower disks that bound the cylinder. The model also calculates the spreading of the upper and lower disks with time. Because the bounding disks of a cylinder are at different altitudes, their spreading is also different and a parcel does not retain its original cylindrical shape. In fact, after t_m for its center particle, a disk is no longer a disk but is represented by a Gaussian particle density distribution with no actual edge or limit. These Gaussian distributions model the fallout as it diffuses outward, but each distribution always remains centered about the particle initially at its center.

Any parcel [actually disk] of fallout that is inside the cloud cap at time t_m is given the stabilization radius R_s. (The difference between t_m and stabilization time is ignored.) For any size particle, the first separation from the cap is taken to occur at time t_i, and this wafer, which initially is at the initial cloud base, is given radius R_i. Its trajectory is followed to cloud stabilization, at which time its height, z_{min}, which may be below ground zero, is recorded. Parcels of fallout of this same particle size at height z are assigned

stabilization radii

$$R = R_i + (R_s - R_i)\frac{z - z_{min}}{z_{B,s} - z_{min}}; \quad z_{min} \leq z \leq z_{B,s} \quad (2.6.8)$$

[note: In the above paragraph the term parcel is used where wafer would have been preferable, in the author's opinion]
Norment states that partitioning the cloud cap into 5 cylinders has been found adequate for all cases that he investigated prior to the publication of his report, but he also gives a formula that can be used as a alternative for selecting the number of cylinders to use,

$$n = 10 + \log_{10}(W) \qquad (2.6.9)$$

A.6 Dispersion by Ambient Turbulence

Following DELFIC, subsequent to t_m, each parcel of fallout is taken to have a Gaussian distribution in the horizontal with variance given by

$$\sigma(t)^2 = \left[\sigma(t_m)^{2/3} + \frac{2}{3}\epsilon^{1/3}(t - t_m)\right]^3; \quad \sigma(t_m) \leq \sigma(t) \leq \sigma_l \quad (2.7.1)$$

$$\sigma(t)^2 = \sigma_l^2 \left\{ 2(t - t_m)\left(\frac{\epsilon}{\sigma_l^2}\right)^{1/3} + 3\left[\frac{\sigma(t_m)^2}{\sigma_l^2}\right]^{1/3} - 2 \right\}; \quad \sigma(t) > \sigma_l \quad (2.7.2)$$

where ϵ is turbulence energy density dissipation rate, σ_l^2 is the parcel variance when its dispersion rate becomes constant, taken to be $10^9 m^2$, and $\sigma(t_m) = R/2$. (The difference between t_m and stabilization time is ignored.)

Using Wilkins' [8] approximation for ϵ, we define an average ϵ

$$< \epsilon >= 0.06/z_m$$

and an average settling time

$$< t >= \frac{z_m}{< f >}$$

where $< f >$ is average settling speed and z_m is the maximum parcel height above ground. Substituting these quantities into Equations (2.7.1) and (2.7.2), we obtain at deposition time, t_d,

$$\sigma(t_d)^2 = \left[\sigma(t_m)^2 + 0.26099\frac{z_m^{2/3}}{< f >}\right]^3;$$

$$z_m^{2/3} \leq 3.83155 < f > [1000 - \sigma(t_m)^{2/3}] \qquad (2.7.3)$$

$$\sigma(t_d)^2 = 7.8297 \times 10^5 \frac{z_m^{2/3}}{< f >} + 3 \times 10^6\, \sigma(t_m)^{2/3} - 2 \times 10^9;$$

$$z_m^{2/3} > 3.83155 < f > [1000 - \sigma(t_m)^{2/3}] \qquad (2.7.4)$$

A.7 Particle Size Distribution, Activity Calculation and Mass of Fallout

A table of 75 particle diameters larger than 50 μm from a set of 100 computed by DELFIC for a lognormal particle number distribution with median diameter 0.407 and geometric standard deviation 4.0 is stored. Corresponding to this table is stored a table of H + 1 hour exposure rate activity fractions calculated by DELFIC for a 0.5 KT fission yield for fission types U238TN and P239HE and averaged.

A fallout prediction may be run using the complete table of 75 particle sizes or it can be run using every other, every third, or every fourth entry. K factors (Roentgens $m^2hr^{-1}KT^{-1}$) for seven fission types also are stored and any one of these may be selected. (see Table 1 in the main body of the text)

If the initial cloud is divided vertically into n fallout parcels for each particle size class, then the area integrated activity at a height of three feet above the ground from an impacted parcel of fallout in the i'th particle size class is

$$Q_i = KW_F F_i \Phi / n \qquad (2.8.1)$$

where W_F is fission yield, F_i is the H + 1 hour exposure rate activity fraction in the i'th particle size class[9] and Φ is a time decay factor. For exposure rate at time t (hours), $\Phi = t^{-1.26}$ and, for integrated exposure (dose) from time t_1 to t_2 (hours), $\Phi = (t_1^{-0.26} - t_1^{-0.26})/0.26$.

To account for the height of burst above ground zero, the fission yield is multiplied by the factor

$$f_d = (0.45345)^{\lambda/65}; \quad \lambda > 0 \qquad (2.8.2)$$

where λ is scaled height of burst in units $ft\, KT^{-1/3}$. This factor is based on a curve of activity fraction down vs. scaled height of burst in Volume 5 of DASA 1251.

The DELFIC formulation for mass of fallout is used,

$$m = 0.07704W^{3/3.4}(360 + \Lambda)(180 - \Lambda)^2; \quad 0 \leq \Lambda \leq 180 \qquad (2.8.3)$$

where W is total yield in KT and Λ is scaled height of burst in units $ft\, KT^{-1/3.4}$ and the mass is in kilograms. This model does not have a subsurface capability.

A.8 Distribution of Grounded Fallout Particles

Following DELFIC, the top and base wafers of each fallout parcel are transported separately to ground impaction. Then the impact point coordinates and variances of the two wafers are combined to form parameters for a bivariate Gaussian function which is used to distribute the parcel mass or activity over the impact plane.

[9]Total fraction of fallout involved in fallout calculations, i.e. the sum of 75 F_i coefficients, is 60.6442% percent of the total activity.

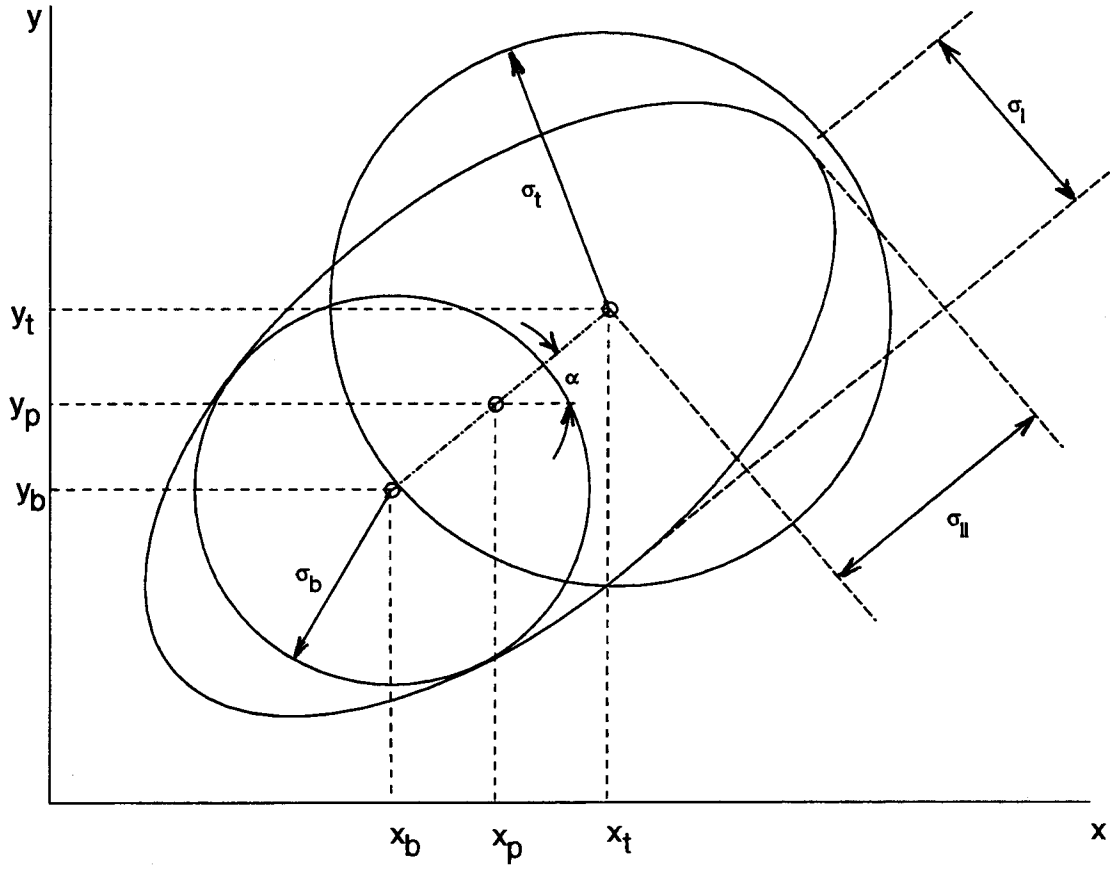

Figure 26: Synthesis of a deposit increment standard deviation ellipse from the impact points and standard deviations of the parcel top and base wafers.

If the total mass or area integrated activity in the parcel is Q, then the mass per unit area or activity contributed by this parcel at point x,y in the impact plane, $\omega(x, y)$ is

$$\omega(x,y) = \frac{Q}{2\pi\sigma_{||}\sigma_{\perp}} \exp\left[-\frac{(X-X_p)^2}{2\sigma_{||}^2} - \frac{(Y-Y_p)^2}{2\sigma_{\perp}^2}\right] \qquad (2.9.2)$$

where

$$\begin{aligned} X &= x\cos(\alpha) + y\sin(\alpha) \\ Y &= y\cos(\alpha) - x\sin(\alpha) \end{aligned} \qquad (2.9.2)$$

and X_p and Y_p are defined similarly. The parcel central coordinates, x_p, y_p, standard deviations, $\sigma_{||}, \sigma_{\perp}$, and orientation angle α are determined from the coordinates and standard deviations of the impacted parcel top and base (subscripts t and b indicate top and base respectively) according to

$$
\begin{aligned}
x_p &= (x_t + x_b)/2 \\
y_p &= (y_t + y_b)/2 \\
r &= \sqrt{(x_t - x_b)^2 + (y_t - y_b)^2}
\end{aligned}
\tag{2.9.3}
$$

$$
\begin{aligned}
\sigma_{||}^2 &= (\sigma_t + \sigma_b + r)^2/4 \\
\sigma_{|}^2 &= \sigma_t \sigma_b
\end{aligned}
\tag{2.9.4}
$$

$$
\begin{aligned}
\cos(\alpha) &= |x_t - x_b| / r \\
\sin(\alpha) &= \frac{(x_t - x_b)(y_t - y_b)}{r\,|x_t - x_b|)}
\end{aligned}
\tag{2.9.5}
$$

A.9 Particle Size Class Data

For completeness, the Fortran data statements specifying the representative particle diameters for the 75 particle size classes, their sea level settling speeds, and their activity fraction coefficients are given below:

```
Particle size (units,  meters)
DATA PD /4.6189E-3,2.7058E-3,1.9869E-3,1.6103E-3,1.3673E-3,
1 1.1937E-3,1.0616E-3,9.5693E-4,8.7138E-4,7.9984E-4,7.3891E-4,
2 6.8627E-4,6.4022E-4,5.9953E-4,5.6326E-4,5.3069E-4,5.0125E-4,
3 4.7449E-4,4.5003E-4,4.2759E-4,4.0691E-4,3.8777E-4,3.7001E-4,
4 3.5348E-4,3.3805E-4,3.2360E-4,3.1005E-4,2.9731E-4,2.8530E-4,
5 2.7397E-4,2.6325E-4,2.5310E-4,2.4347E-4,2.3433E-4,2.2562E-4,
6 2.1733E-4,2.0943E-4,2.0188E-4,1.9466E-4,1.8775E-4,1.8114E-4,
7 1.7480E-4,1.6871E-4,1.6287E-4,1.5725E-4,1.5184E-4,1.4664E-4,
8 1.4163E-4,1.3680E-4,1.3213E-4,1.2763E-4,1.2328E-4,1.1908E-4,
9 1.1501E-4,1.1107E-4,1.0725E-4,1.0355E-4,9.9963E-5,9.6483E-5,
A 9.3105E-5,8.9825E-5,8.6638E-5,8.3541E-5,8.0529E-5,7.7599E-5,
B 7.4748E-5,7.1972E-5,6.9268E-5,6.6632E-5,6.4063E-5,6.1558E-5,
C 5.9112E-5,5.6725E-5,5.4394E-5,5.2116E-5/

Sea level settling speeds (units  meters/second)
DATA FO/18.113,13.661,11.319,9.8484,8.7798,7.9459,7.2655,6.6946,
1 6.2047,5.7777,5.4005,5.0641,4.7612,4.4867,4.2363,4.0067,3.7952,
2 3.5996,3.4180,3.2490,3.0911,2.9433,2.8045,2.6741,2.5512,2.4351,
3 2.3254,2.2216,2.1230,2.0295,1.9406,1.8560,1.7754,1.6987,1.6253,
4 1.5553,1.4884,1.4244,1.3631,1.3044,1.2482,1.1943,1.1426,1.0930,
5 1.0453,.99953,.95559,.91335,.87274,.83359,.79600,.75981,.72501,
6 .69145,.65912,.62795,.59793,.57242,.54529,.51590,.48642,.45791,
7 .43340,.40902,.38555,.36297,.34125,.32037,.30031,.28107,.26261,
8 .24492,.22799,.21180,.19633/

Activity fractions
DATA AA/.005826,.005980,.006088,.006170,.006240,.006303,.006361,
1.006415,.006467,.006516,.006564,.006611,.006656,.006701,.006745,
2.006788,.006831,.006874,.006916,.006959,.007001,.007043,.007086,
3.007128,.007170,.007213,.007256,.007299,.007343,.007387,.007431,
4.007456,.007521,.007567,.007613,.007660,.007708,.007756,.007805,
5.007854,.007905,.007956,.008009,.008062,.008116,.008172,.008228,
6.008286,.008344,.008405,.008466,.008529,.008594,.008660,.008728,
7.008798,.008870,.008944,.009020,.009099,.009180,.009263,.009350,
8.009439,.009532,.009628,.009728,.009832,.009940,.010053,.010171,
9.010294,.010423,.010558,.010701,.010851/
```

B Input Instructions for SIMFIC

The copy of the SIMFIC code used in this report came without instructions and had no documentation within the code describing the input. Because the process of unscrambling the input was time consuming, what was learned is recorded here for the benefit of anyone wanting to run SIMFIC in the future. Users should be be cautioned that only a few of the code options were exercised in the process of the present study so the accuracy and completeness of these instructions has never been verified. SIMFIC was written at a time when the norm was to run codes by submitting a deck of punched cards. As a result, the input records are usually limited to eighty characters. The numbered items below represent the different input data records. Each data set includes one of each record from 1 through 7, as many type 8 records as there are wind data points, and one each of 9 and 10.

1. A record used as a title for the run, format 18A4

2. Device parameters, location and time format 5f10.0, A6

   W the yield in kilotons

   FW the fission yield in kilotons

   ZGZ altitude of ground zero, meters

   HOB height of burst above ground zero, meters

   TGZ time of shot detonation, seconds and defaults to 0

   FISSID ASCI variable describing device type, e.g. P239HE

3. ASCII variable array **MCCHAR(20)**, format 20A1. This array gets parsed into a logical variable array, **MC**. All elements of **MCCHAR** that are t or T translate into true, and all other characters get translated into a logical false.

   MC(1) if true, then the user specifies the map size and grid increments.

   MC(2) controls whether or not to output wind information. False gets you lots of output.

   MC(3) if true you output information on wind layer base data

   MC(4) if true output summed weighted wind data

   MC(5) if true prints out the total activity in each particle size class over one square meter of ground.

   MC(6) Selects whether to calculate the map point Gaussians by an exact (true) or approximate (false) technique.

   MC(7) if true and both MC(8) and MC(9) are false, use 2 as the particle size class skip parameter.

   MC(8) if true and MC(9) is false, use 3 as the particle size class skip parameter.

MC(9) if true use 4 as the particle size class skip parameter.
if **MC(7)** **MC(8)** and **MC(9)** are:

- FFF use all size classes
- TFF use skip parameter = 2
- xTF use skip parameter = 3, (x means either T or F)
- xxT use skip parameter = 4

MC(10) if false use 5 cloud subdivisions in the vertical. If true calculate the number of cloud subdivisions (10+log(W)).

MC(11) – MC(20) do not appear to be used.

4. **FORM**, a character variable, format(A4), that must be either METE or RESO. If it is METE, the wind is input as direction and velocity. If it is RESO the wind is input as X (east) and Y (north) velocity components.

5. **FMT**, a character variable, format (20A4), that specifies the format to use for reading in the wind data, e.g. (F12.0,24X,2F12.0). Wind data records have three floating point data fields.

6. **SCALE**, an 5 element array of scale factors, format (5F10.0)
Used for scaling the inputs in the wind records, which is very convenient if the raw data is given in mks units. If left blank defaults for elements 1,2, and 3 are 1.0, and for elements 4 and 5 are 0.

   SCALE(1) Scale factor for altitude to get it into meters. If you input altitude in feet, then you'd want **SCALE(1)**=3.28.

   SCALE(2) Scale factor for speed to get it into m/s. If you input speed in ft/s you'd want **SCALE(2)**=.3048.

   SCALE(3) Scale factor for direction to convert input to degrees.

   SCALE(4) Offset for altitude. If wind speeds are given AGL (above ground level), then you'd input the elevation of ground zero here in the same units as you used to input the altitude.

   SCALE(5) Is an angular offset for the wind direction inputs. It should be in the same units as the wind direction inputs (usually degrees).

7. **N1, N2, N3** Integers defining the order of wind data input, format 3I4

   N1 Tells which data field on the wind input records is the altitude. If it's the first data field, **N1** is 1.

   N2 Specifies which data field on the wind cards is the angle (if **FORM**=METE) or the easterly wind component of the wind velocity vector (if **FORM**=RESO).

   N3 Specifies which data field on the wind cards is the speed (if **FORM**=METE) or the norterly wind component of the wind velocity vector (if **FORM**=RESO).

8. **AP(1), AP(2), AP(3)** are the altitude, wind direction and speed (if **FORM**=METE); or the altitude, and wind X and Y components (if **FORM**=RESO). Which **AP** corresponds to which quantity is specified by record 7. An indefinite number of records are read. What signals a stop is a record giving an altitude value greater than or equal to 999999. Format is specified by **FMT** defined in record 6.

9. Record specifying the type of calculation desired and some input parameters for the calculation, format(I2, 1X, A1, 1X, 2A1, 3X, 7F10.0)

   MREQ An integer variable. Valid values are 1 to 18 inclusive. The meanings are deciphered from the hollerith parts of the format statements in subroutine MAPSF.

   - 1 – A strange one. A "count of contributing deposit increments."
   - 2 – Exposure rate normalized to H + 1 hour. R/HR
   - 3 – Exposure rate at time T1. R/HR
   - 4 – Exposure rate normalized to H+1 hour from particles in the size range T1 to T2. R/HR
   - 5 – Exposure accumulated between T1 and inf. R
   - 6 – Exposure accumulated between T1 and T2. R
   - 7 – Exposure accumulated between T1 and T2 assuming all particles are on the ground at T1. R
   - 8 – Exposure accumulated between T1 and inf. assuming all particles are on the ground at T1. R
   - 9 – Appears to be the same as 5.
   - 10 – Appears to be the same as 6.
   - 11 – Total Mass/area of contributing deposit increments. Kg/m^2
   - 12 – Mass/area deposited between T1 and T2. Kg/m^2
   - 13 – Mass/area deposited by particles in size range T1 to T2. Kg/m^2
   - 14 – Does not appear to be used.
   - 15 – Time of onset of fallout deposition. s
   - 16 – Time of cessation of fallout deposition. s
   - 17 – Diameter of smallest deposition particle. microns
   - 18 – Diameter of largest deposition particle. microns

   MBOUNC A string variable turned into a logical variable. If **MBOUNC** is T or t, then a bunch of stuff related to calculating map grid points, increments and min/max values may be skipped.

   CPNTCH Jetsam. It is defined and then appears only in declaration statements.

   CPNCCH Jetsam again. It is defined and then appears only in declaration statements.

   T1 Depending on the type of calculation can be a start time in hours or a particle size in meters. Not always needed.

T2 Depending on the type of calculation can be an end time in hours or a particle size in meters. Not always needed.

GRUFF A combined ground roughness and radiation meter response factor (default factor = 1.0). Normally use 0.5 for comparisons with NTS above ground test data.

10. Record to control locations at which output is desired, (8f10.0). This record is used if **MC(1)** is true.

XMIN Map parameter. Minimum easte on map. m

XMAX Map parameter. Maximum easterly point on map. m

YMIN Map parameter. Minimum northerly point on map. m

YMAX Map parameter. Maximum northerly point on map. m

DGX Spacing between easterly grid points m

DGY Spacing between northerly grid points m

********** SIGN CONVENTION **********

For a wind blowing from south to north, the wind direction is 180 degrees, i.e. the wind direction differs by 180 degrees from the wind velocity vector.

****

SIMFIC data sets seem to be stackable. The program is setup to read an indefinite number of data sets. To end the process include two blank records after the last data set.

C Input Data Used in Calculations for Tests

Event Name	Total Yield (kilotons)	Fission Yield (kilotons)	HOB (meters)	Altitude of Ground Zero (meters)
Small Boy[10]	low	low	3.048	938.2
Johnie Boy	0.5	0.5	0	1570.6
Jangle Sugar	1.2	1.2	1.07	1284.7
Koon	150.	150.	4.145	0.0
Zuni	3380.		2.743	0.0

Table 6: Nuclear Test Input Data

Small Boy			Johnie Boy			Buster Jangle Sugar		
Altitude (m) ASL	Azimuth Degrees	Speed m/s	Altitude (m) ASL	Azimuth Degrees	Speed m/s	Altitude (m) ASL	Azimuth Degrees	Speed m/s
938.2	255.	0.4	1580.6	195.	3.6	1294.7	190.	.9
1219.2	255.	0.9	1828.8	170.	3.6	1828.8	170.	6.7
1524.	255.	1.8	2133.6	160.0	3.6	2438.4	180.	13.4
1828.	255.	2.7	2438.4	160.	5.7	3048.	200.	16.5
2133.6	255.	3.6	2743.2	160.	8.2	3657.6	200.	18.8
2438.4	250.	3.1	3048.	170.	7.7	4267.2	210.	20.6
2743.2	240.	6.3	3352.8	180.	6.2	4876.8	210.	22.8
3048.	240.	8.0	3657.6	180.	7.7	5486.4	200.	32.2
3657.6	240.	4.0	3962.4	190.	8.9	6096.	200.	27.7
4267.2	240.	4.0	4267.2	200.	10.8	7620.	210.	31.7
4876.8	240.	4.0	4572.	200.	11.3	9144.	210.	35.8
5486.4	280.	7.2	4876.8	200.	11.3	10668.	210.	40.2
6096.	280.	13.0	5181.6	200.	13.9			
			5486.4	200.	13.9			
			5791.2	210.	13.4			
			6096.0	200.	11.8			

Table 7: Weather Data for Small Boy, Johnie Boy, and Buster Jangle Sugar

[10]Numerical values for yield have not yet been declassified and so are not given here.

Koon			Zuni		
Altitude (m) ASL	Azimuth Degrees	Speed m/s	Altitude (m) ASL	Azimuth Degrees	Speed m/s
10.	40.	10.3	10.0	50.0	9.8
304.8	70.	8.9	304.8	80.0	11.6
609.6	60.	8.	609.6	70.0	11.2
914.4	90.	4.	914.4	70.0	12.5
1219.2	120.	3.6	1219.2	90.0	12.5
1524.0	140.	4.5	1524.0	90.0	10.7
1828.8	170.	6.3	1828.8	100.0	9.8
2133.6	170.	8.9	2133.6	100.0	9.8
2436.4	190.	7.2	2438.4	100.0	9.8
2743.2	200.	7.2	2743.2	100.0	9.8
3048.0	200.	7.2	3048.0	100.0	10.3
3657.6	180.	8.9	3657.6	90.0	10.7
4267.2	200.	4.0	4267.2	90.0	7.6
4572.0	200.	4.5	4572.0	100.0	6.7
4876.8	190.	5.4	4876.8	110.0	5.4
5486.4	200.	5.4	5486.4	100.0	5.4
6096.0	220.	2.2	6096.0	140.0	5.4
7620.0	190.	10.3	7620.0	160.0	8.0
9144.0	210.	11.2	9144.0	170.0	6.3
10668.	210.	14.3	10668.0	220.0	13.0
12192.	230.	17.4	12192.0	220.0	20.6
13716.	280.	12.5	13716.0	210.0	17.9
15240.	240.	17.9	15240.0	240.0	13.0
15849.	230.	20.1	15544.8	250.0	13.0
			16764.0	240.0	1.3
			18288.0	80.0	7.6
			19812.0	90.0	13.4
			21336.0	90.0	13.4
			22860.0	90.0	17.9
			24384.0	100.0	21.5
			25908.0	100.0	21.5
			27432.0	100.0	21.5

Table 8: Weather Data for Koon and Zuni

D Distribution List

1 Bradley A. Clark
X-DO, MS 8218
Los Alamos National Laboratory
Los Alamos, NM 87545

1 Don Daigler
US Department of Energy
Nevada Operations Office
P.O. Box 98518
Las Vegas, NV 89193-8518

1 William Hartman
37241 Canyon View Drive
Tuscon, AZ 85739

1 Joseph McGahan
Science Applications International Corp.
1710 Goodridge Dr.
Box 1303 MS T91
Mc Lean VA, 99102

1 Thomas J. Sullivan
LLNL/ARAC Program
P.O. Box 808
Livermore, CA 94551-0808

1 Fred L. Wasmer
1158 County Road 1200 East
Champaign, IL 61821

1 John A. Weidner
MS DP-23
US Department of Energy, Headquarters Germantown
19901 Germantown Road
Germantown, MD 20874-1290

1 Gary Worth
P. O. Box 1663 MS J562
Los Alamos NM 87545

2 Atomic Weapons Establishment, Aldermaston
Building SB46.1D
Attn: Doug Thompson, John Marriage
Reading, Berkshire RG74PR
U.K.

1 MS 0405 Dave Carlson
1 0557 T. J. Baca
5 0557 M. J. Sagartz
1 0557 T. W. Simmermacher
1 0766 D. M. Ellis
10 0767 B. A. Boughton
10 0767 D. B. Clauss
1 0767 F. Harper

1	0767	M. E. Larsen
1	0767	B. Marshall
1	0767	R. K. Wilson
1	1221	H. Season
1	9052	L. Baxter
1	9018	Central Technical Files, 8940-2
5	0899	Technical Library, 4916
2	0619	Review and Approval Desk, 12690 For DOE/OSTI